Weather and Climate Extremes 32 (2021) 100319

Contents lists available at ScienceDirect

Weather and Climate Extremes

journal homepage: http://www.elsevier.com/locate/wace

Updated analysis of gauge-based rainfall patterns over the western tropical Pacific Ocean

Joshua J. Wimhurst *, J. Scott Greene **

Department of Geography and Environmental Sustainability, University of Oklahoma, Norman, OK, 73019, USA

ARTICLE INFO

Keywords:
Tropical Pacific Ocean
Comprehensive Pacific Rainfall Database (PACRAIN)
Rainfall observations
Interdecadal Pacific Oscillation
Global Precipitation Climatology Project (GPCP)

ABSTRACT

This work considers observed changes in tropical Pacific Ocean rainfall amounts and the influence of climate variability cycles upon them. Observations were taken from the Comprehensive Pacific Rainfall Database (PACRAIN), using strict data selection criteria of >99% data completeness from eight locations for the period 1971–2017. These data were used to analyze temporal and spatial rainfall patterns based on several indicators that considered rainfall amount and frequency, 95th percentile extreme rainfall events, and length of consecutive rain/drought events. These indicators were also computed using satellite-derived observations from the Global Precipitation Climatology Project (GPCP), as a means to compare gauge-based values with nearby estimates from the GPCP product. Results show a temporal pattern that tended towards a reduction in rainfall amounts and frequency across the tropical Pacific Ocean. The impact of phase changes of the Interdecadal Pacific Oscillation (IPO) was also examined. There was some evidence of the impact of the IPO, as well as of the El-Niño Southern Oscillation (ENSO), when seasonal and monthly trends in these indicators were analyzed. Comparison of the temporal patterns observed from the rain gauges with the trends computed using the GPCP estimates showed inconsistencies that varied considerably when comparing trends calculated at different island locations. Future work should consider further comparison of GPCP and gauge-based rainfall trends, as well as the attribution of climate change and other climate variability cycles to these trends.

1. Introduction

1.1. Scope of the current study

There has been much concern in recent decades regarding changes in global rainfall patterns. These changes have been in part attributed in some locations to observed increases of global average temperature, which are known to affect water transportation within the hydrological cycle, and therefore the temporal and spatial distribution of rainfall (Trenberth, 2011). Changes to the spatial and temporal patterns of rainfall are vital to understand from the perspective of planning and management of water resources, especially for vulnerable nations that struggle to meet water demands for economic productivity and domestic demand (Greene et al., 2007).

One such vulnerable location is the tropical Pacific Ocean. Many of the Small Island Developing States in this region depend largely on exports of agricultural goods and natural resources to maintain their economies, so a long-term change in rainfall patterns poses a palpable threat. This threat is a consequence of much of the Pacific islands' agriculture being rain-fed, thus making them more prone to impacts of long-term changes in rainfall amount and variability. As such, studies have sought to quantify observed changes in total tropical Pacific rainfall amounts, as well as duration of droughts/floods and extreme rainfall events. Some of these studies used a large geographical scope, such as work by Kruk et al. (2014) that analyzed changes across the entire Pacific Ocean over the 20th Century. Other rain gauge-based studies focused exclusively on the tropical Pacific Ocean. McGree et al. (2014) looked at changes in rainfall amounts at 68 rain gauges from 1961 to 2011 in island groups across the Western Pacific Ocean. Despite largely inconsistent rainfall trends across the region of study, there was evidence for statistically significant ($p < 0.05$) reductions in rainfall amounts of up to 450 mm decade^{-1} in the subtropical South Pacific over the observational period. Similar results have also been identified by studies that have examined smaller geographical regions, such as a study by Frazier and Giambelluca (2016) that considered rain gauge observations in the Hawaiian Islands from 1920 to 2012. This study showed

* Corresponding author.
** Corresponding author.
E-mail addresses: Joshua.J.Wimhurst-1@ou.edu (J.J. Wimhurst), jgreene@ou.edu (J.S. Greene).

https://doi.org/10.1016/j.wace.2021.100319
Received 28 October 2020; Received in revised form 28 February 2021; Accepted 12 March 2021
Available online 15 April 2021
2212-0947/© 2021 The Author(s). Published by Elsevier B.V. This is an open access article under the CC BY license (http://creativecommons.org/licenses/by/4.0/).

rainfall reductions to have occurred across 90% of the islands' land area, particularly on the western half of Hawaii Island itself, possibly due to a significant increase in volcanic haze.

The current study is a successor to Greene et al. (2007), continuing their work in analyzing rain gauge-based historical tropical Pacific rainfall trends and considering their relationship with climatological features, such as the Interdecadal Pacific Oscillation (IPO) and the El Niño-Southern Oscillation (ENSO). Given the concerns of rain gauges being susceptible to various measurement errors, and the potential inaccuracy in using them to infer rainfall trends across larger domains, this study has chosen to compare these rain gauge-based observations to outputs from the Global Precipitation Climatology Project (GPCP), a dataset that combines rainfall observations taken from satellites and rain gauges (Adler et al., 2003). The intent of the current study is therefore to update and refine studies of rain gauge-based historical rainfall trends, by combining an analysis of several rainfall indicators with an adequately strict data completeness criterion, whilst also comparing these results to those obtained from a secondary data source, i.e. the GPCP product.

1.2. Literature overview

There have been previous studies conducted over the last 20-plus years that examined rain gauge-based rainfall trends across the tropical Pacific Ocean. Morrissey and Graham (1996), for example, examined rainfall trends obtained from 250 atoll and island-based locations across the tropical Pacific Ocean from 1971 to 1990. Results from Griffiths et al. (2003) very much agreed with those of Morrissey and Graham (1996), having used rain gauge observations from 1961 to 2000 to find increases in rainfall predominating over the central tropical Pacific, with reductions further to the south. This study, along with more recent examples such as Greene et al. (2007) and McGree et al. (2014), commonly examine long-term rainfall trends using a range of indicators alongside changes in monthly or annual rainfall amount, such as extremes in rainfall frequency and amount, and consecutive days with and without rainfall. Such analysis affords a more holistic picture of historical rainfall climatology across the tropical Pacific Ocean. For instance, Greene et al. (2007) found that reductions of annual rainfall amount occurred consistently to the south of the tropical Pacific Ocean, as also observed by Griffiths et al. (2003) and Morrissey and Graham (1996). This latter study also found these reductions to be simultaneously associated with a decrease in the frequency of rainfall events and an increase in the proportion of rain that falls during heavier rainfall events, thus attesting to a pattern of a reducing annual rainfall amount occurring in heavier, shorter periods of time. However, these older studies possess shortcomings that condone an update to historical rainfall trends over this region, whether being a lack of enlisted observations beyond the year 2000 (Greene et al., 2007), data completeness criteria not being strict enough to capture true observed rainfall trends (e.g. McGree et al. (2014) using a completeness criterion of 80%), or the study's observational period being relatively short (i.e. shorter than a climatological period of 30 years) owing to limited rain gauge observations (Morrissey and Graham 1996).

The decision to use rain gauges in studies of tropical Pacific rainfall trends is motivated by two factors, one being their ability to measure rainfall amounts directly (Bell and Kundu 2003), as well as rain gauges being associated with well-understood measurement errors (Greene et al., 2008). Rain gauges placed on low-elevation islands, such as the many atolls of the tropical Pacific Ocean, are also known to effectively represent open ocean rainfall trends (Lavoie 1963; Janowiak et al., 1994; Morrissey et al., 1994), hence their common usage in this region. This effectiveness can be attributed to land-based rainfall being more susceptible to orographic influences, something that open ocean rainfall does not experience due to lack of high elevation (Morrissey et al., 1995). The ability of atoll-based rain gauges to better represent open-ocean rainfall trends has led to some studies, such as Greene et al. (2007), selecting datasets based on rain gauge elevation as a proxy for orographic effect potential. Several studies have, conversely, attested to the influences of orography on rainfall trends across the Pacific Ocean. Salinger et al. (1995) found in their use of principal component analysis that historical rainfall trends across the islands of and surrounding New Zealand were not consistent with each other, which the authors partially attributed to local orographic differences. Similar patterns have been observed over more tropical locations. Across Hawaii for example, Frazier and Giambelluca (2016) identified varying spatial patterns of rainfall trends across different orographic conditions and also across different climate forcings, such as different ENSO phases.

This orographic influence also exists for much smaller islands. Hopuare et al. (2015) examined observed rainfall amounts from 1961 to 2011 at nine rain gauges across French Polynesia, and found that the effects of orography on the island of Tahiti are sufficient to produce notable differences in rainfall amounts on the island's windward and leeward sides, with the former experiencing larger inter-annual amounts during El Niño events. Despite these aforementioned studies attesting to orographic effects potentially having an important influence on long-term oceanic rainfall trends, the magnitude of this influence could be somewhat limited. In their analysis of several indicators of rainfall trends using rain gauge observations, Griffiths et al. (2003) found a lack of statistically significant differences ($p < 0.05$) in rainfall trends recorded on tropical Pacific atolls versus larger islands, regardless of the indicator enlisted. This result supports the usage of rain gauges to assess long-term rainfall trends in this region, since observations collected on larger and/or more elevated islands still seem to represent these trends effectively, hence their inclusion in more recent studies such as McGree et al. (2014).

Although there are good reasons to use rain gauges as a data source for analysis of rainfall trends, they do possess notable drawbacks, such as their small spatial coverage and the consequent need to infer rainfall trends in the gauges' surroundings (Bell and Kundu 2003). A common alternative in capturing long-term rainfall trends is therefore to enlist observations collected by satellites. The Tropical Rainfall Measuring Mission (TRMM) is an example of a rainfall measuring product that existed to collect satellite-based observations of rainfall over the planet's lower latitudes (NASA TRMM, 2015). Satellites' greatest advantages over rain gauge-based observations are the consistency of their spatial and temporal coverage when measuring rainfall amounts, and the elimination of error from human sources, or ground-based sources such as wind and evaporation (Maggioni et al., 2016). For this reason, satellites have been used to characterize rainfall trends over the tropical Pacific Ocean in many previous studies. Luchetti et al. (2016) describe the use of outputs from two years of PERSIANN-CDR infrared satellite observations, in order to create an atlas of rainfall changes associated with ENSO for a collection of Pacific islands. Many other satellite-based studies concerning the nature of tropical rainfall trends have also focused on a few years of observations. Adler et al. (2000) enlisted outputs from TRMM to illustrate changes in global rainfall patterns (in mm day^{-1}) during and following the 1998 El Niño event, and Sorooshian et al. (2002) enlisted two years of outputs from PERSIANN-CDR to describe diurnal variability of rainfall patterns at various locations across the tropics.

More pertinently to the current study, satellite observations have been occasionally used to describe rainfall patterns over longer periods of time. However, satellites are often limited by the short length of their observational records, therefore limiting their suitability for illustrating such long-term rainfall trends (Hughes 2006). Satellites are also prone to underestimating extreme rainfall amounts, as mentioned by Kruk et al. (2015) in their study of satellite-based Pacific Ocean rainfall trends from 1988 to 2012. This study of extreme rainfall frequency found statistically significant increases ($p < 0.05$) to have occurred in the western tropical Pacific, with smaller decreases in the central and eastern tropical Pacific. This result is not consistent with that of Greene et al. (2007), a study that evaluated the same indicator using rain gauges. It should be

clarified that these two studies did not possess the same observational periods, allowing climate variability cycles to potentially explain the difference between them. As such, it is common practice for studies that examine satellite-based rainfall trends to corroborate results using rain gauge observations (Bowman 2005; Hughes 2006; Salio et al., 2015). This approach provides an opportunity in the current study to not only update the region's rain gauge-based rainfall trends, but also to compare results using two different rainfall measurement approaches.

Several studies of tropical Pacific rainfall trends (Greene et al., 2007; McGree et al., 2014; Kruk et al., 2015) have sought to describe the climatology of rainfall observations and subsequently suggest processes within the climate system that could be contributing to these trends. Rainfall amounts across the tropical Pacific Ocean are greatly influenced by the Inter- Tropical Convergence Zone (ITCZ), a band of near-equatorial deep convection that produces notably heavy rainfall. The ITCZ's mean state is one of remaining slightly to the north of the equator (Raymond et al., 2003). Annual variation at this latitude occurs due to hemispheric differences in energy content (Broccoli et al., 2006; Kang et al., 2008; Schneider et al., 2014), which is amplified by the water vapor positive feedback process (Clark et al., 2018). The ITCZ itself responds to several cycles within the climate system. For instance, the variability of the East Pacific segment of the ITCZ is influenced greatly by the near-monthly westerly passage of the Madden-Julian Oscillation (Raymond et al., 2006), as well as the interannual enhancement/inhibition of its amplitude of convection in response to El Niño/La Niña events (Xie et al., 2018). Kim et al. (2020) have also identified a relationship between the IPO and the ITCZ, noting a "strengthening of the ITCZ over the warm tropical Pacific and a weakening over the Atlantic and northern Brazil during DJFMAM, associated with the IPO pattern." Changes in the ITCZ have important implications for the rainfall patterns of tropical Pacific islands in the longer term as well. Studies of the ITCZ's response to climate change have shown global temperature increases to be associated with a narrowing (Byrne and Schneider 2016) of the convergence zone itself, as well as a strengthening of the ITCZ's deep convection (Bony et al., 2013). These studies of ITCZ dynamics collectively attest to its importance in producing trends in tropical Pacific rainfall amounts, which would be especially valid if the expected changes in ITCZ width, strength, and latitude in response to climate change can be seen in rain gauge or satellite-based observations.

It is important to note, however, that the ITCZ's influences on rainfall are perhaps more important for the northern half of the tropical Pacific Ocean, given its typical latitudinal position over this region remaining between 2°N and 9°N in recent years (Schneider et al., 2014). Rainfall trends in the southern half of the tropical Pacific Ocean, especially its western side, are largely influenced by movements of the South-Pacific Convergence Zone (SPCZ; Folland et al., 2002; Vincent et al., 2011; McGree et al., 2016). Furthermore, changes in tropical Pacific sea surface temperatures (SSTs) in part caused by the IPO result in a multi-decadal shift of SPCZ position and associated rainfall (Wang and Picaut 2004). It was found by both Salinger et al. (2001), and Folland et al. (2002) that the IPO's positive phase (SST increase) is associated with a north-east shift of the SPCZ, with negative IPO phases producing a south-west shift. Although the periodicity of the IPO is on the order of decades, it has been shown to have powerful effects on the global climate, with work by Meehl et al. (2013) noting that the current negative phase of the IPO is related to the deceleration of average global temperature increase that was observed in the early 2000s.

2. Materials and methods

2.1. Data sources

The tropical Pacific rainfall observations enlisted in the current study were taken from the Comprehensive Pacific Rainfall Database (PACRAIN) – a metadata system that compiles rainfall totals from hundreds of sites across the tropical Pacific Ocean. PACRAIN is updated every month with newly collected quality controlled rainfall observations (PACRAIN 2018; Cook and Greene 2019). The sources that comprise PACRAIN's metadata are obtained from several meteorological institutes around the Pacific Ocean (Morrissey et al., 1995). These sources include:

- The New Zealand National Institute of Water and Atmospheric Research, Ltd.
- The French Polynesian Meteorological Service.
- The National Center for Environmental Information (NCEI, formerly the National Climatic Data Center (NCDC)).

A fourth rainfall data source, which is unique to PACRAIN, is the Schools of the Pacific Rainfall Climate Experiment (SPaRCE), which gives educational institutions around the Pacific Ocean the equipment to measure rainfall amounts (Postawko et al., 1994). The combination of several data sources in a region that previously possessed sparse weather observations is a significant reason for PACRAIN's popularity in studies of tropical rainfall trends. The number of observation locations within its metadata system has increased from around 250 in the 1990s (Morrissey et al., 1995) to over 1 100 today (PACRAIN 2018). One of the hallmarks of PACRAIN, however, is the rigor of the quality control when new data are uploaded. See PACRAIN (2018), Greene et al. (2007), Greene et al. (2008) or Cook and Greene (2019) for details about PACRAIN's data quality control.

Rainfall observations were taken from locations with records that possessed 99% or greater data completeness (the criterion used by Greene et al. (2007)) from January 1st, 1971 to December 31st, 2017, where data completeness refers to the percentage of days between 1971 and 2017 for which rainfall observations at a given location were taken. This range of years allows for maximum representation of rainfall trends that have happened during this time domain, and also exceeds the minimum 30-year period recommended to account for climate variability cycles that could affect tropical Pacific Ocean rainfall (World Meteorological Organization 2011).

Such a strict data completeness criterion is enlisted in the current study in order to eliminate concerns regarding elongated observational gaps, as well as to better facilitate calculation of extreme rainfall indicators. This criterion does limit the number of locations within the PACRAIN database eligible for the current study to eight, which is undeniably a small sample of observations for quantifying tropical Pacific rainfall trends. However, lowering the data quality criterion would jeopardize the integrity of the research and of the identified patterns. Elevation of these gauges was not a criterion used when selecting locations to analyze, since orographic effects on these islands were found by Griffiths et al. (2003) to not significantly alter measured rainfall amounts. Given the current study's interest in relating observational trends to phases of the IPO (among other processes of the climate system), it is also worth mentioning that this observational period contains a full positive (1978–1998) and negative (1999–2013) IPO phase (Meehl et al., 2016). As such, much of the results presented in the current study shall focus on these two time frames as well as trends over the entire observational period of 1971–2017.

The small number of rain gauge locations that meet the data completeness criterion of the current study heightens the concerns of using rain gauges to suggest historical rainfall trends across large spatial domains, as well as the need to include observations from a secondary source. Selection of GPCP as the secondary source was based on its extensive use as a well-established satellite-derived and gauge-enhanced rainfall product (Huffman et al., 1997). Daily rainfall observations over the tropical Pacific Ocean were taken from the GPCP's tertiary 1° latitude x 1° longitude product, with data available from January 1997 to present. Whilst this period is shorter than the available rain gauge record, it is enough to cover the period of the IPO's recent negative phase (Meehl et al., 2016), meaning that the available GPCP data can be used to corroborate the spatial patterns indicated by rain gauge observations

over this period of time.

2.2. Methods used

The names, units, and definitions of the indicators used in this study are summarized in Table 1. Rainfall Amount and Rainfall Frequency are standard indicators that give a general overview of how rainfall patterns across the tropical Pacific Ocean have changed between 1971 and 2017. Further information comes from analyzing extreme rainfall events, since they may affect rainfall amounts over the region more significantly, and thus are the events in which leaders, policy planners, and local communities would be the most interested. As such, analyses of the frequency, intensity, and proportion of extreme rainfall events and their trends were also conducted. Definitions of these indicators, as well as rainfall amount and rainfall frequency, are the same as those used in Griffiths et al. (2003) and Greene et al. (2007). In these definitions, a 95th percentile rainfall event refers to (approximately) the 18th wettest day in a given year, the 5th wettest day in a given season, or the 2nd wettest day in a given month. Since these indicators offer no suggestion of changes in the severity and duration of droughts and rainfall events, the indicators known as Maximum Dry/Wet Consecutive Days were also analyzed in this study, using the same definitions as in McGree et al. (2014), where "measurable amount of rainfall" refers to rainfall amounts that are greater than 1 mm of rainfall in a given day.

Much like Greene et al. (2007), this study computed trends across these seven indicators by considering them as changes per year (i.e., mm yr^{-1}, days yr^{-1}, % yr^{-1}) at each of the eight rain gauge locations. Trends in these indicators were considered monthly and seasonally as well as annually, with the intention of revealing patterns that are perhaps negated by considering only annual temporal scales. These trends are presented as spatial maps of the tropical Pacific Ocean from 1971 to 2017, in which changes in rainfall pattern indicators at each location are represented by a triangle that is proportional to the magnitude and sign of these changes. White triangles are indicative of trends that are statistically significant at the 90% confidence level ($p < 0.1$), such that an indicator at a given location experiences a change that is significantly different than zero. Statistical significance at each location or grid point was determined based on Spearman's Rho least-squares regression analysis, a rank-order, non-parametric test of a given rainfall indicator (Yue et al., 2002).

An option in studies such as the current study is to conduct a field significance test, in which statistical significance is decided by the number of points in a location that possess significance exceeding the number expected based on random chance (Li et al., 2018). However, the current study is not attempting to assert widespread spatial significance based on the results of each rain gauge location/grid point, only whether historical trends in rainfall indicators exist or have persisted when compared to those of previous work. Thus, field significance tests are not necessary for this study and have not been conducted.

The current study also examines the relationship between trends in these rainfall indicators and the climate system processes that are known to influence them, namely the IPO and ENSO. As such, two sets of annual and seasonal maps were created using each of the seven indicators, both for changes during the IPO's positive (1978–1998) and negative phases (1999–2013) that fell within the observational period. The same analysis was also conducted using the GPCP data, with the results presented as tables showing the magnitude and sign of the trends in all seven indicators, as well as their differences from their corresponding rain gauge trends, in order to facilitate comparison between these two sources of rainfall observations. This comparison was only made over the IPO's negative phase, given the limitations of the GPCP observational record. For determination of the relationship between Table 1's indicators and ENSO, trends in indicators were broken down by month and presented as time series plots from 1971 to 2017. Due to the exceedingly large number of possible graphs and maps of different combinations of years, seasons, months, phases, and indicators, figures presented in the main text are those that best summarize the results of the analysis of the gauge and GPCP products.

Table 1
Summary of the rainfall trend indicators enlisted for this study.

Indicator	Unit	Definition
Rainfall Amount	mm	Physical amount of total rainfall in a given year from 1971 to 2017
Rainfall Frequency	days	Number of days on which there is a non-zero amount of rainfall in a given year from 1971 to 2017
Extreme Rainfall Frequency	days	Number of days on which the amount of rainfall is greater than the location's average 95th percentile amount in a given year from 1971 to 2017
Extreme Rainfall Intensity	mm	Physical amount of rainfall during ≥95th percentile events in a given year from 1971 to 2017
Extreme Rainfall Proportion	%	Percentage of rainfall that occurs during ≥95th percentile events in a given year from 1971 to 2017
Maximum Wet Consecutive Days	days	Greatest number of days for which measurable rainfall (>1 mm) does occur in a given year from 1971 to 2017
Maximum Dry Consecutive Days	days	Greatest number of days for which measurable rainfall (>1 mm) does *not* occur in a given year from 1971 to 2017

3. Results

3.1. Annual trends in rainfall patterns

Rainfall trends at each of the eight rain gauge locations were analyzed based on the seven selected indicators enlisted in the current study (see Table 1). Due to the lack of spatial coverage over the Tropical Pacific Ocean that these rain gauges afford, care must be taken to not overstate the significance of trends observed at individual or several rain gauge locations. Furthermore, the triangles in these maps represent differing quantities, even when considering a single indicator, hence each map has a unique legend. Figs. 1–3 present maps of annual rain gauge trends over the three observational periods (1971–2017, positive IPO, and negative IPO) for Rainfall Amount, Rainfall Frequency, and Maximum Dry Consecutive Days respectively. Statistically significant ($p < 0.1$) changes in these indicators at individual locations are identified by white triangles, of which there are few in Fig. 1. Despite this lack of statistical significance, consistent decreases of Rainfall Amount occurred at the majority of locations, especially during the negative IPO phase (Fig. 1c), with all locations but American Samoa attesting to a reduction in Rainfall Amount at this time. Note, however, that American Samoa is a geographic outlier, so that might be a partial cause of the difference in the patterns. These decreases persist throughout the positive IPO phase as well (Fig. 1b), reaching values as much as -45 mm yr^{-1} at Palau, the only location that possessed a statistically significant change in rainfall during this phase. This overall reduction weakens when considering the entire observational period, with five out of eight locations signaling a decrease in Rainfall Amount. Greene et al. (2007) and McGree et al. (2014) also both found that decreases of Rainfall Amount were dominant over this region, especially towards the south and west.

The trends in Rainfall Frequency are somewhat similar to those for Rainfall Amount, as shown in Fig. 2. Decreases in Rainfall Frequency occurred at all locations except for Kwajalein in the positive IPO phase (Fig. 2b), with some indication of increases in Rainfall Frequency during the negative IPO phase (Fig. 2c). The trends in the negative phase also seem to be much stronger than those in the positive phase, reaching up to -3 days yr^{-1} at Kwajalein and $+3$ days yr^{-1} at Palau and American Samoa, with the increasing trends at these latter two locations possessing statistical significance. The overall patterns across both phases seem to be largely cancelled out when considering the entire observational period (Fig. 2a), in which no Rainfall Frequency trends exceeded

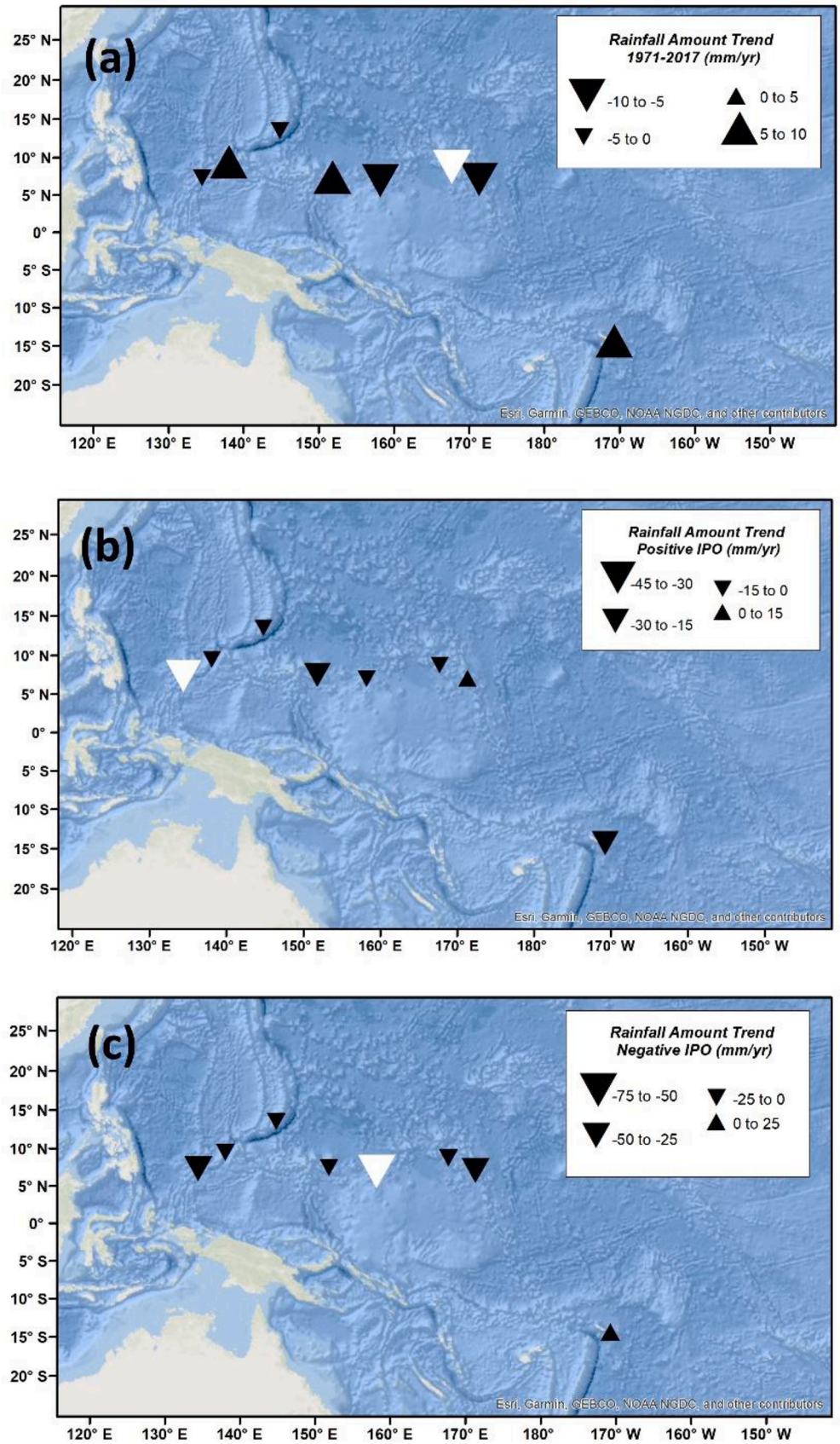

Fig. 1. Maps showing annual trends in Rainfall Amount (in mm yr^{-1}) at all rain gauge stations over the entire observational period (a), as well as the positive (b) and negative (c) IPO phase durations. White triangles indicate trends that are statistically significant ($p < 0.1$). *Gauge locations from left to right: Palau, Yap, Guam, Chuuk, Pohnpei, Kwajalein, Majuro, and American Samoa.* "Oceans" basemap for all relevant figures from ESRI (2018).

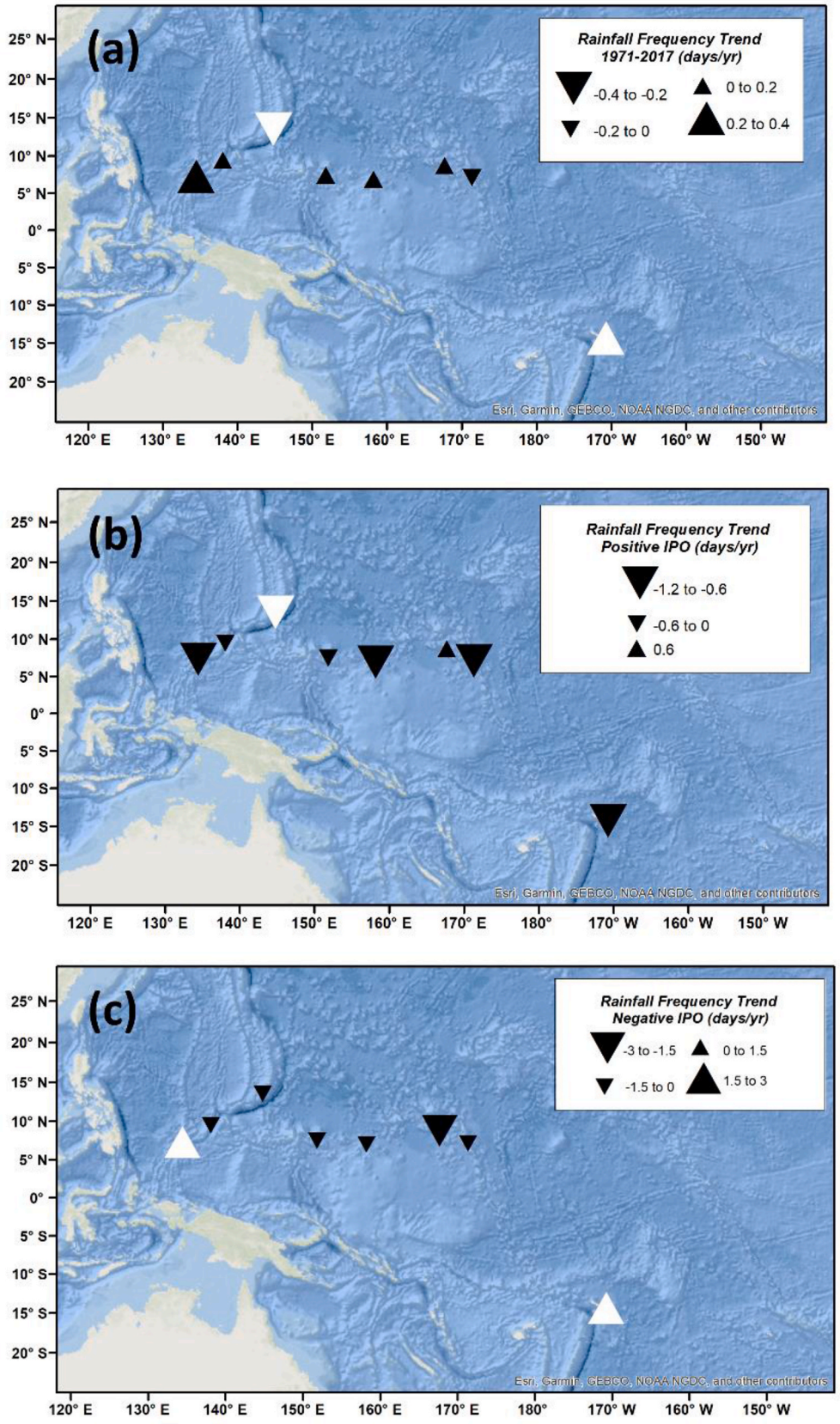

Fig. 2. Same as Fig. 1 but for rainfall frequency.

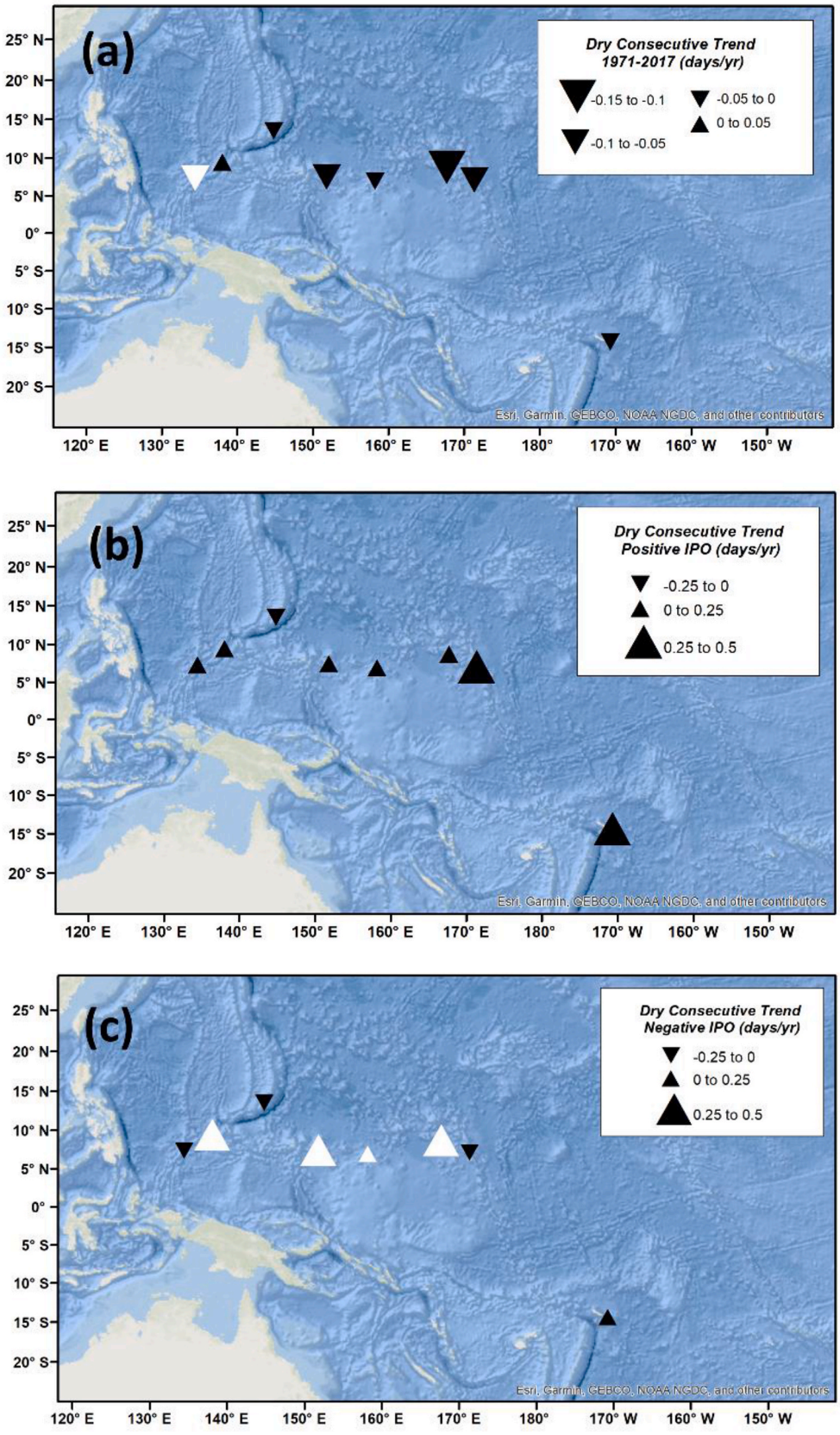

Fig. 3. Same as Fig. 1 but for maximum dry consecutive days.

± 0.4 days yr^{-1}. However, the strength of the Rainfall Frequency trends within individual IPO phases show potential for serious short to medium-term water management implications, with the sign of the Rainfall Frequency trends at individual locations during the positive IPO phase possessing consistency with previous work (Greene et al., 2007). Rainfall Amount and Rainfall Frequency are good indicators of overall rainfall pattern changes over the Pacific Ocean, hence the focus on these indicators in the current study.

Annual trends for the other indicators show some evidence of being stronger in the negative IPO phase than in any other observational period, such as reductions of Extreme Rainfall Frequency reaching up to -0.8 days yr^{-1} at Pohnpei ($p < 0.1$). However, the gauge-based trends using these indicators generally lacked statistical significance, also often lacking consistency of sign and magnitude between proximal islands. Maximum Dry Consecutive Days is the only remaining indicator that produced trends that were either spatially consistent or statistically significant, as shown in Fig. 3. Most locations have experienced an increase in this quantity across both IPO phases, with any decreases being smaller in magnitude. These increases in days without rainfall reached up to $+0.5$ days yr^{-1}, with these increases being statistically significant during the negative IPO phase (Fig. 3c) at Yap, Chuuk, Pohnpei, and Kwajalein. This result is opposite in sign to that of McGree et al. (2014), but their work analyzed trends in this indicator decadally rather than annually, thereby perhaps erasing smaller temporal scale changes. The effects of the IPO again appear to be somewhat diminished, based on the lack of change of trend direction between the two phases. What Fig. 3 does highlight, nevertheless, is a notable and spatially consistent increase in the number of consecutive days without rainfall recorded at tropical Pacific islands and atolls in the last several decades, indicating a drying of this region. The drying could be an overall consistent pattern, or possibly could be associated with an increase in wet season rainfall and a decrease in the dry season.

3.2. Seasonal trends in rainfall patterns

One of the main concerns with presenting trends in rainfall indicators annually is elimination of trends that happen on smaller temporal scales. For example, the wind direction changes associated with ENSO typically begin and are most prevalent in Northern Hemisphere (NH) winter and spring (Wang and Picaut 2004). The rainfall pattern

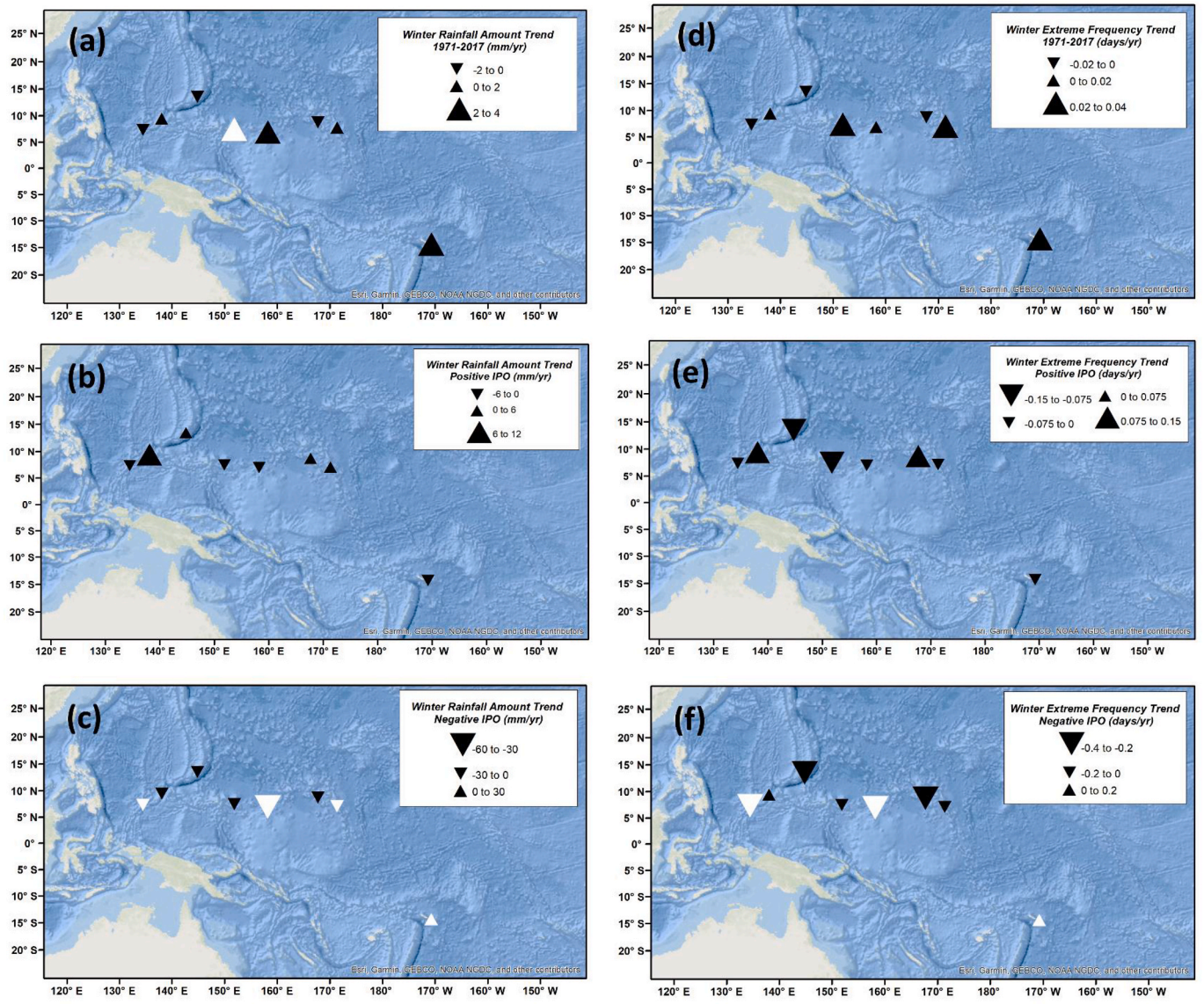

Fig. 4. Maps showing winter trends in Rainfall Amount (a, b, c) and Extreme Rainfall Frequency (d, e, f) at all rain gauge stations over the entire observational period (a, d) as well as the positive (b, e) and negative (c, f) IPO phase durations. White triangles indicate trends that are statistically significant ($p < 0.1$).

changes associated with this event could be harder to identify if only annual trends in rainfall indicators are considered, hence the utility of examining seasonal trends (as well as monthly trends, see Section 3.3). Figs. 4–7 present maps of observed changes in rainfall indicators for NH winter, spring, summer, and autumn respectively, in the same fashion as the maps discussed in Section 3.1. For each season, results from two of the seven rainfall indicators have been presented, based on the statistical significance of results at individual locations or consistent spatial/temporal patterns (e.g. the trends shown for 1971–2017 matching more closely to one of the two IPO phases).

In the case of most rainfall indicators, but especially Rainfall Amount and Extreme Rainfall Frequency (Fig. 4), NH wintertime reductions were strongly favored during the negative IPO phase (Fig. 4c, f). This was especially true in Pohnpei, where the reduction in Rainfall Amount during this 14-year phase measured up to −60 mm yr^{-1}, a result that possessed statistical significance along with those of Palau, Majuro, and American Samoa. It is also apparent from Fig. 4 that, despite the consistency of the signs of these rainfall indicators during the negative IPO phase, many of these trends become much weaker or even become increases when considering the entire observational period (Fig. 4a, d). This also suggests that there is perhaps an IPO signal in the mean state of the precipitation patterns as well. Given the tendency of these winter trends to be of opposing signs in different IPO phases, such as those of Palau, Guam, Majuro, and American Samoa, this weaker trend for the observational period could be a consequence of trends in the two IPO phases being cancelled out by each other. This potential influence of the IPO is consistent with previous literature's expectations of the IPO's influences on tropical Pacific rainfall (Salinger et al., 2001; Folland et al., 2002), a finding that was more difficult to detect when considering annual trends in these indicators (Fig. 1). Another result of interest from these NH winter trends was lower magnitudes when compared to annual trends of the same indicators, with the latter possessing trends up to three times greater in magnitude, especially when considering Extreme Rainfall Intensity and Maximum Dry Consecutive Days. This tendency for seasonal trends to be smaller in magnitude than those of annual trends, particularly for the positive IPO phase and the entire observational period, was true of all seasons.

Differences between seasonal and annual trends also existed when considering seasons other than winter. Trends in Rainfall Amount and Extreme Rainfall Proportion in NH spring (Fig. 5) illustrate two interesting results that characterized this season. Firstly, there is some evidence for an east-west spatial pattern in these two rainfall indicators. This finding is especially true for Extreme Rainfall Proportion during the negative IPO phase (Fig. 5c) and Rainfall Amount during the positive

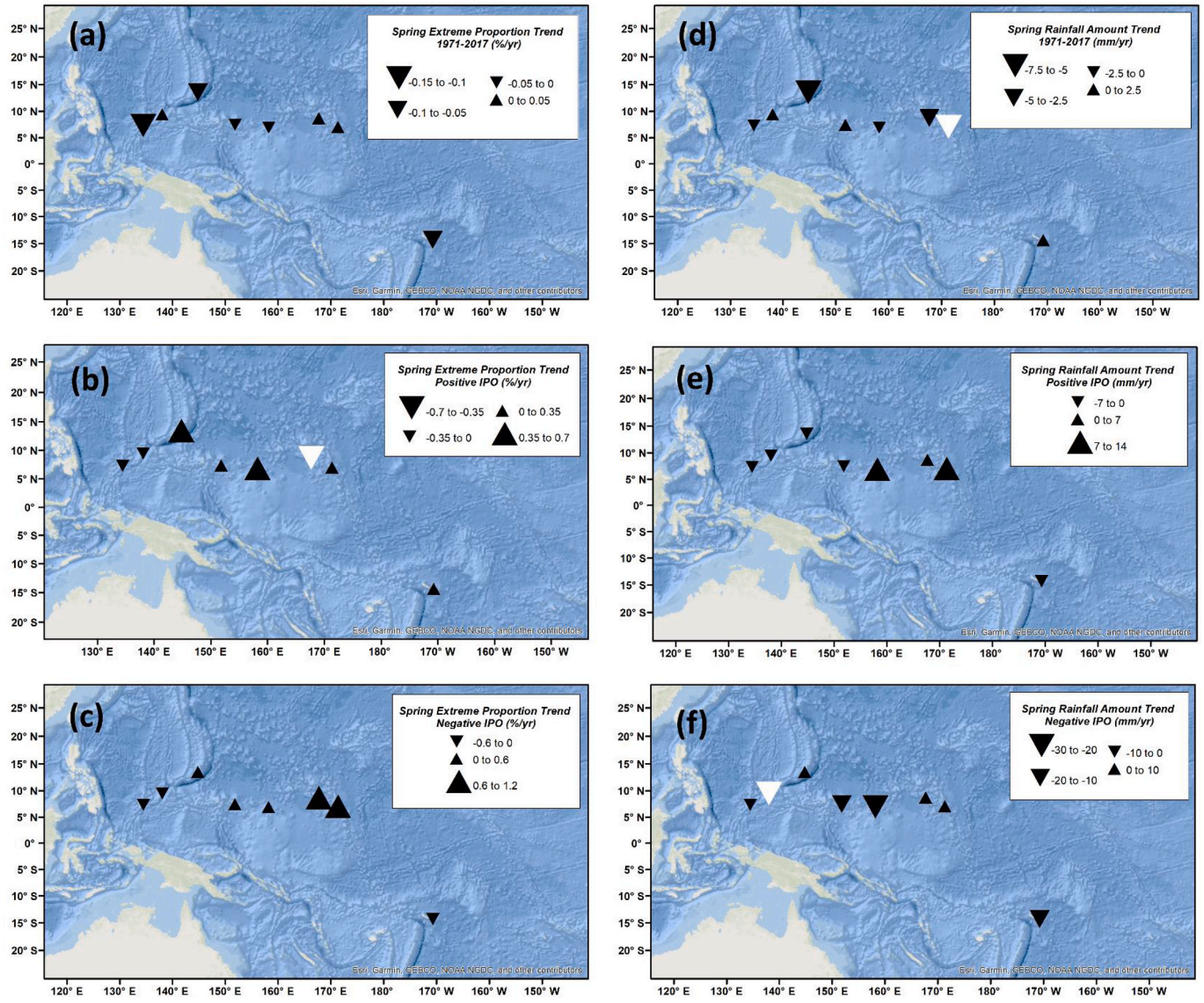

Fig. 5. Same as Fig. 4, but for spring trends in Extreme Rainfall Proportion (a, b, c) and Rainfall Amount (d, e, f).

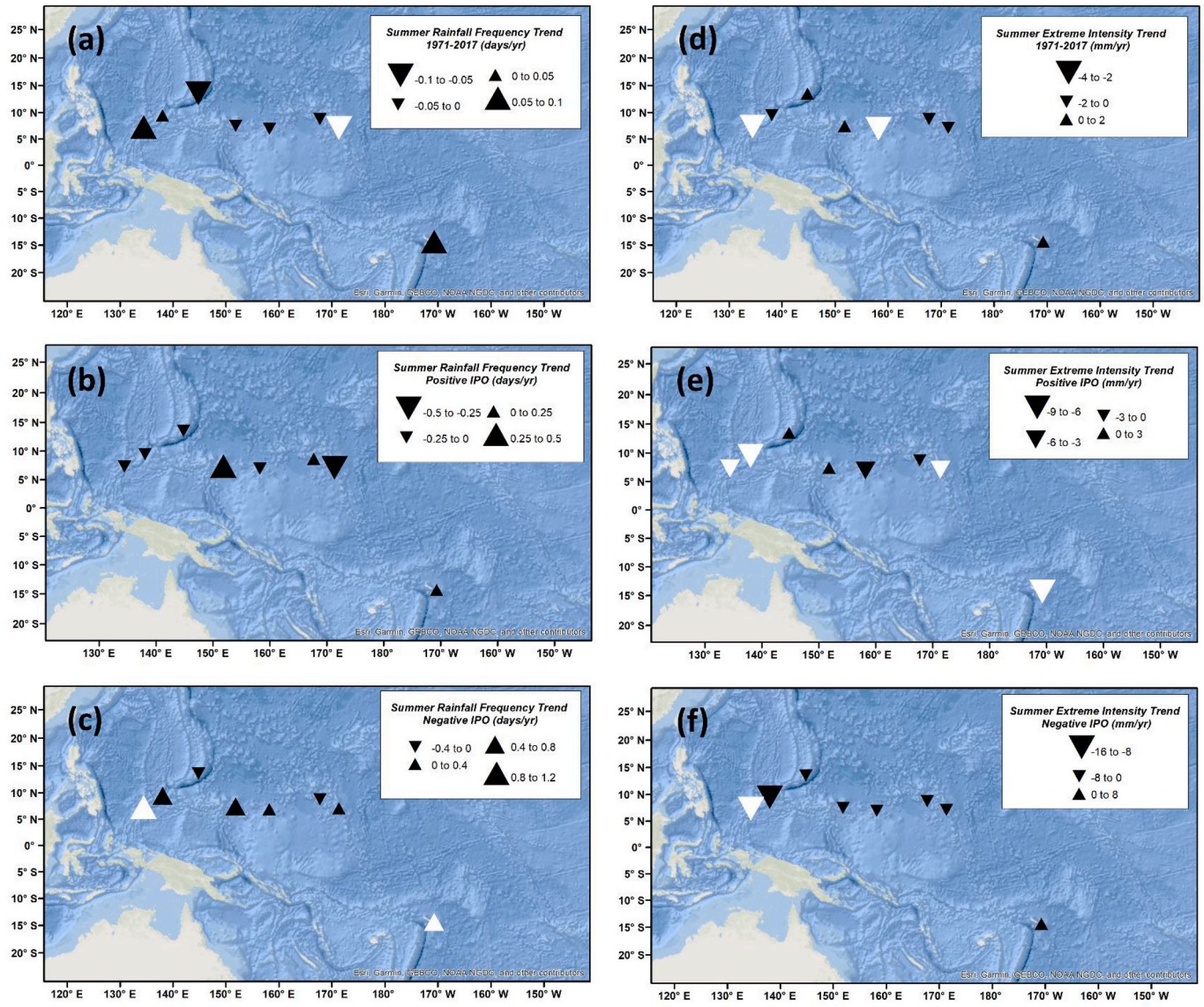

Fig. 6. Same as Fig. 4, but for summer trends in Rainfall Frequency (a, b, c) and Extreme Rainfall Intensity (d, e, f).

phase (Fig. 5e). In both maps, weak reductions in these indicators are prevalent to the west of the tropical Pacific Ocean, with stronger increases further eastward. Given the association of changes to the ENSO index with changes in rainfall patterns (Wang and Picaut 2004), such a zonal gradient in rainfall is perhaps expected, but could also have happened randomly due to lack of spatial coverage afforded by rain gauges and/or the lack of statistically significant results (discussed further below).

A result that occasionally appeared in this seasonal analysis is rainfall indicator trends over the entire observational period being more consistent with those of one IPO phase over another. This result was especially true of Extreme Rainfall Intensity in the NH summer (Fig. 6), in which seven out of eight rain gauge locations possessed the same sign when comparing maps for the entire observational period (Fig. 6d) and the positive IPO phase (Fig. 6e), with the magnitude range for the latter being slightly larger perhaps because of the negative IPO phase (Fig. 6f) moderating trends from 1971 to 2017. However, it is more common for trends in individual IPO phases (across all seasons) to have little to no similarity with trends over the entire observational period. This finding might indicate that the phases of the IPO have had little influence on historical rainfall trends over the tropical Pacific Ocean in the last few decades.

A final result of interest when considering seasonal trends is the magnitude of trends produced for the same indicators in different seasons. Fig. 7 shows the historical trends for Rainfall Frequency (Fig. 7a–c) and Extreme Rainfall Frequency (Fig. 7d–f) in NH autumn. An obvious feature of these maps is the lack of statistically significant results at individual locations, especially over the entire observational period. Upon closer inspection, this lack of significant trends can be attributed to the small changes in these indicators that have taken place, such as Rainfall Frequency changing by no more than ± 0.08 days yr^{-1} from 1971 to 2017 (Fig. 7c). Contrast this result with those of other seasons, such as the range of ± 0.15 days yr^{-1} in NH spring (not shown), and it becomes apparent that the magnitude of this indicator can differ greatly between different seasons. This result highlights the importance of examining seasonal as well as annual trends in the data. Seasonal comparisons between IPO phases attest to a similar result, with positive IPO Maximum Wet Consecutive Days ranging from -0.15 to 0.05 days yr^{-1} in NH spring versus ± 0.25 days yr^{-1} in autumn (not shown). It is of interest that recent changes in rainfall indicators have possessed notable seasonal differences. Such a result is perhaps expected, given the seasonal to inter-annual cycles of features that influence tropical Pacific rainfall, such as the ITCZ (Broccoli et al., 2006) and ENSO (Gouriou and Delcroix 2002), are known to possess.

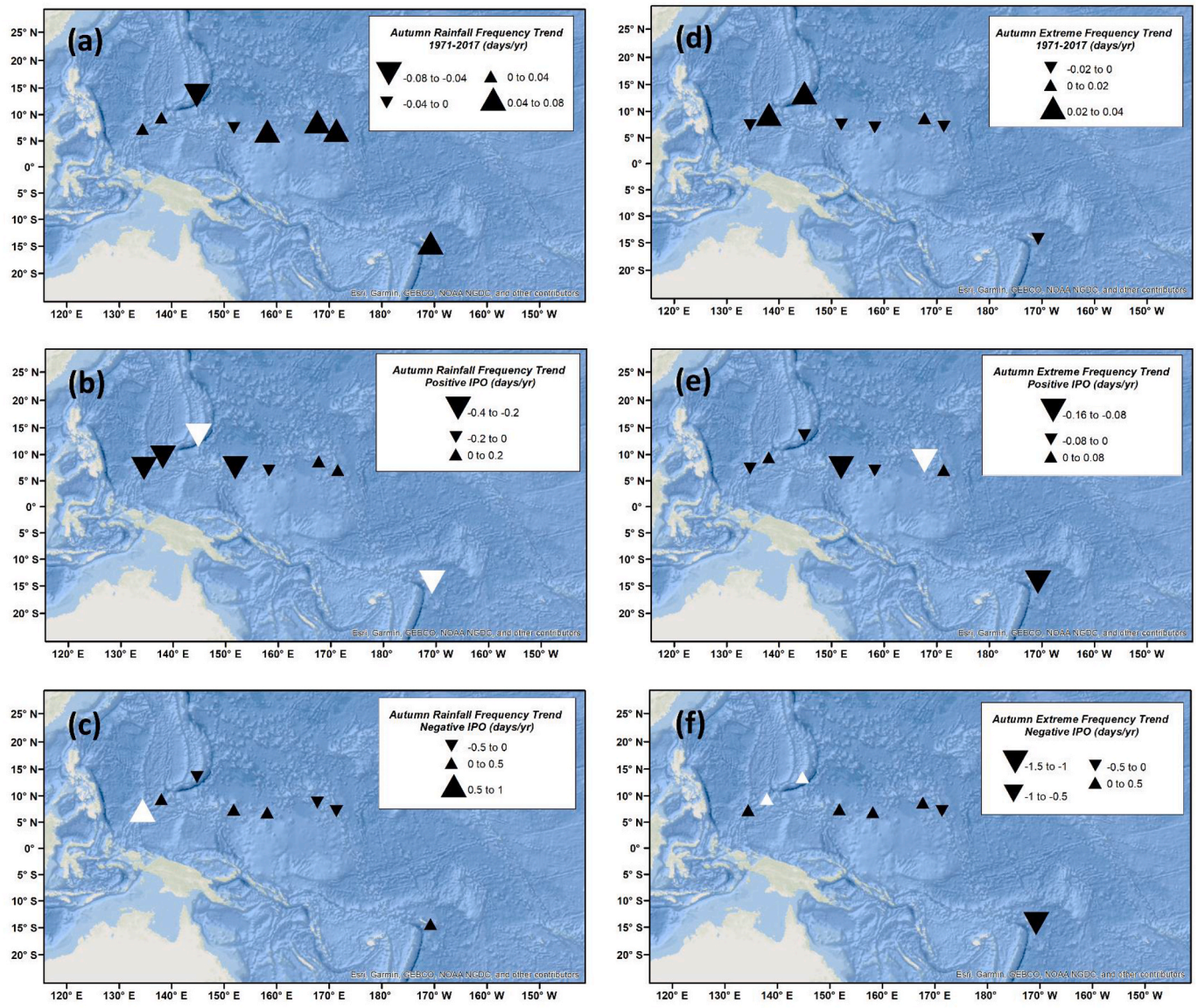

Fig. 7. Same as Fig. 4, but for autumn trends in Rainfall Frequency (a, b, c) and Extreme Rainfall Frequency (d, e, f).

3.3. Monthly trends in rainfall patterns

As with Section 3.2, breaking down changes in rainfall indicators using smaller temporal scales facilitates identification of trends that may otherwise be obscured, especially those that are non-random ($p < 0.1$). Time series plots were therefore generated for selected months in which a statistically significant change in a given indicator and rain gauge location occurred between 1971 and 2017. By presenting these monthly trends in this manner, it is possible to distinguish individual years that make the largest contributions to changes in these indicators, such as years that experience an El Niño or La Niña event. Seasonal data may show smoother patterns, but analysis of monthly precipitation makes it easier to identify specific sub-patterns and changes within the data. Of the 87 time series plots that possessed statistically significant changes for a given location, month, and rainfall indicator, 60 exhibited a decreasing trend. Given the prevalence of these negative, non-random trends, it is perhaps less surprising that annual changes in some of these rainfall indicators presented overall decreases at the majority of rain gauge locations (Figs. 1–3). Fourteen of these non-random time series trends are shown in Fig. 8, based on their ability to best summarize the results of this section of the current study.

The first notable result from these time series plots is, regardless of the month, location, and indicator considered, each of these trends possesses distinguishable inter-annual variability. This variability occasionally presents itself as a multi-annual oscillation, such as for Maximum Dry Consecutive Days on Yap in April (Fig. 8h) and Extreme Rainfall Proportion on Palau in May (Fig. 8l). There is also arguable evidence of the effects of ENSO on these indicators, such as the high Extreme Rainfall Intensity in June on Yap in 1982 (Fig. 8j) coinciding with a strong El Niño event, as does the anomalously high Maximum Wet Consecutive Days in August on Majuro in 2002–03 (Fig. 8f). This result is to be expected, since ENSO index shifts have been observed to coincide with simultaneous annual-scale shifts in rainfall amount and location, such as that associated with the ITCZ (Xie et al., 2018), as well as the SPCZ to the south of these rain gauges (Folland et al., 2002; Gouriou and Delcroix 2002; Vincent et al., 2011). However, despite two notable El Niño events having occurred in 1997–98 and 2015–16 (Kumar and Chen 2017), the presumed impacts of these events on tropical Pacific rainfall patterns seem to be largely absent from Fig. 8's time series plots. However, we note that care is needed when interpreting El Niño events, since their signals are often the largest toward the end of the first year of such an event. Nevertheless, there is some

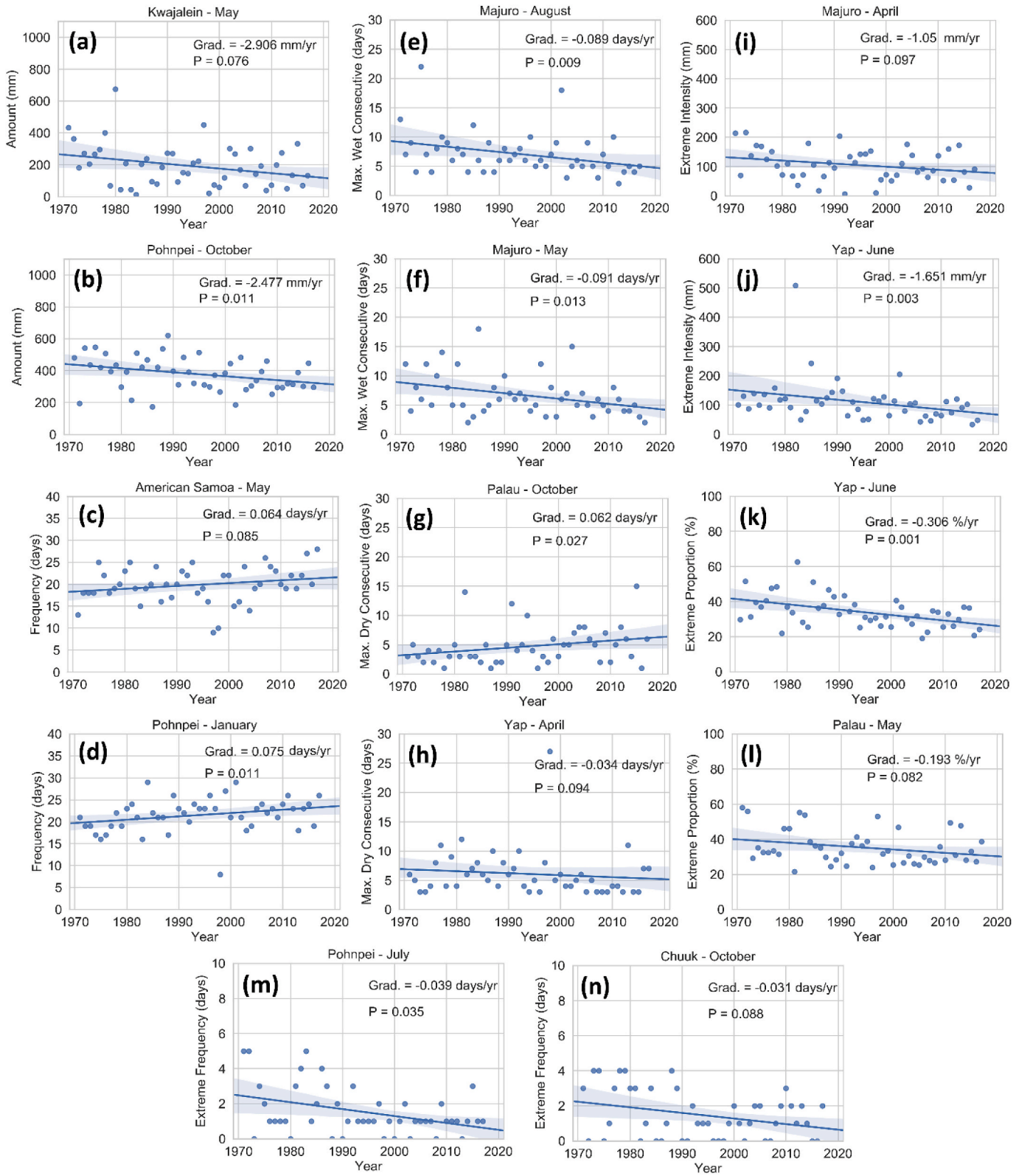

Fig. 8. Time series plots that show trends in the rainfall indicators in the current study when broken down by month and by gauge location. Each plot's regression line and confidence interval (blue shading) indicate statistically significant relationships ($p < 0.1$), based on a Spearman's Rho test. Indicators are presented as follows: Rainfall Amount (a, b), Rainfall Frequency (c, d), Maximum Wet Consecutive Days (e, f), Maximum Dry Consecutive Days (g, h), Extreme Rainfall Intensity (i, j), Extreme Rainfall Proportion (k, l), and Extreme Rainfall Frequency (m, n). (For interpretation of the references to colour in this figure legend, the reader is referred to the Web version of this article.)

evidence for anomalously high Rainfall Amount totals over Kwajalein in May in these El Niño years (Fig. 8a), but such time series plots are in the minority. The effects of ENSO on tropical Pacific Ocean rainfall are perhaps limited on multidecadal timescales (i.e. from 1971 to 2017), even when examining trends in rainfall indicators by month.

This time-series analysis also suggests that ENSO's effects are inconsistent over individual tropical Pacific islands, with single El Niño/La Niña events being unable to explain long term changes such as decreasing Rainfall Amount or Extreme Rainfall Proportion. However, the effects of ENSO on inter-annual variability of these rainfall indicators is still of note, even if its effects are not consistently dominant, which agrees with findings from McGree et al. (2014). Moreover, the effects of the IPO on these monthly measures of rainfall indicators also seem to be limited, despite the multidecadal timescale of these time series plots. This is evident from the direction of the interannual variability that these plots possess, which given the presupposed influence of the IPO on tropical Pacific rainfall should have changed sometime in the late 1990s (Meehl et al., 2016). The importance of stochastic rainfall variability and climate variability cycles being unable to fully explain the trends of these time series plots shall be discussed further in Section 4.

3.4. Comparing rain gauges and GPCP outputs

As stated in Section 1.2, it is common practice for studies of gauge-based rainfall measurements to enlist satellite-derived observations in order to compare the results from the different measurement systems (Bowman 2005; Hughes 2006; Salio et al., 2015). As such, the current study enlisted tropical Pacific rainfall observations from the GPCP (Adler et al., 2003), which combines satellite and rain gauge-derived observations into a single composite dataset. Rather than compute simple differences in measured rainfall, since such analysis has been covered by the aforementioned literature, annual and seasonal trends in the seven rainfall indicators were calculated using GPCP data and presented in Table 2 and Appendix A1-4 respectively. These trends were calculated at GPCP model grid points in proximity to each rain gauge location over the duration of the IPO's most recent negative phase (1999–2013), such that the four grid points within 1° latitude and 1° longitude of each rain gauge location were selected. The focus on the negative IPO phase was motivated by the GPCP's limited data availability, as well as the objective of comparing these trends to those of rain gauge data (which are also shown in these tables) over a consistent time frame. When comparing datasets, it is important to note the difference in the types or products. Sun et al. (2017) examined 30 currently available global precipitation data sets, including gauge-based, satellite-related, and reanalysis data sets. They noted "large differences in both the magnitude and the variability of precipitation estimates" and also especially, "Large differences in annual and seasonal estimates were found in tropical oceans." As Sun et al. (2017) identify, "reliability of precipitation data sets is mainly limited by the number and spatial coverage of surface stations, the satellite algorithms, and the data assimilation models." Similarly, it has been shown repeatedly in the statistical and climatological literature that, as King et al. (2013) point out, "gridded dataset[s] tend to underestimate the intensity of extreme heavy rainfall events and the contribution of these events to total annual rainfall as well as overestimating the frequency and intensity of very low rainfall events."

When considering Table 2 (annual rainfall trends), it is interesting to analyze both the extent of difference (gauge value minus GPCP value) between GPCP and rain gauges in calculating rainfall indicators, as well as the sign of the differences that occur. As before, assigning large-scale spatial significance to these results is inappropriate due to the small number of rain gauges enlisted. Furthermore, assessment of climatology based on the findings of these tables was avoided, since these trends had been computed from 14 years of rainfall observations. The indication from Table 2 is relatively sporadic occurrences of high or low agreement between rainfall indicator trends produced by GPCP and rain gauges. For instance, indications on American Samoa are that the difference between the rain gauges and the GPCP product for the Maximum Dry Consecutive Days trend is up to −2 (−1.972) days yr^{-1}. This difference is

Table 2
Observed annual changes in the seven rainfall indicators around each rain gauge location, using GPCP observations. The difference between the GPCP-derived values and each respective rain gauge is given, with values for both datasets taken over the duration of the IPO's recent negative phase (1999–2013). Yellow GPCP cells indicate trends that are statistically significant ($p < 0.1$).

Station Name	Latitude	Longitude	Rainfall Amount (mm/yr)		Rainfall Frequency (days/yr)		Max. Consecutive Wet Days (days/yr)		Max. Consecutive Dry Days (days/yr)		Extreme Rainfall Frequency (days/yr)		Extreme Rainfall Intensity (mm/yr)		Extreme Rainfall Proportion (%/yr)	
			GPCP	Gauge-GPCP	GPCP	Gauge-GPCP	GPCP	Gauge-GPCP	GPCP	Gauge-GPCP	GPCP	Gauge-GPCP	GPCP	Gauge-GPCP	GPCP	Gauge-GPCP
Chuuk	6.5	151.5	-19.78	2.09	0.471	-0.571	-0.532	0.504	-0.125	0.432	-0.232	0.193	-4.471	-1.223	-0.012	0.07
	6.5	152.5	-12.98	-4.71	0.478	-0.578	0.089	-0.117	0.092	0.215	-0.196	0.157	-2.354	-3.34	0.018	0.04
	7.5	151.5	-24.89	7.2	0.314	-0.414	0.175	-0.203	-0.017	0.324	-0.517	0.478	-4.882	-0.812	0.022	0.036
	7.5	152.5	-25.99	8.3	0.11	-0.21	-0.378	0.35	0.142	0.165	-0.517	0.478	-3.818	-1.876	0.065	-0.007
Guam	13.5	144.5	-8.236	-9.114	-0.925	0.775	0.039	-0.131	-0.05	0.004	0.06	-0.085	1.744	-10.279	0.383	-0.358
	13.5	145.5	-9.746	-7.604	-1.114	0.964	0.503	-0.595	-0.142	0.096	0.089	-0.114	-0.107	-8.428	0.329	-0.304
	14.5	144.5	1.064	-18.414	-1.682	1.532	0.342	-0.434	0.489	-0.535	0.504	-0.529	2.387	-10.922	0.204	-0.179
	14.5	145.5	-2.152	-15.198	-1.596	1.446	-0.1	0.008	0.764	-0.81	0.032	-0.057	1.123	-9.658	0.204	-0.179
Palau	6.5	133.5	32.68	-69.37	0.732	1.722	0.175	0.114	-0.092	-0.118	0.325	-0.925	2.827	-34.547	-0.215	-0.322
	6.5	134.5	23.05	-59.74	1.121	1.333	0.214	0.075	0.214	-0.424	-0.021	-0.579	0.781	-32.501	-0.196	-0.341
	7.5	133.5	14.5	-51.19	0.225	2.229	0.346	-0.057	0.01	-0.22	0.046	-0.646	2.561	-34.281	-0.067	-0.47
	7.5	134.5	13.8	-50.49	0.05	2.404	-0.142	0.431	0.157	-0.367	0.121	-0.721	1.129	-32.849	-0.107	-0.43
Kwajalein	8.5	167.5	-19.84	2.02	-1.336	-0.185	-0.139	0.146	0.035	0.425	-0.132	-0.028	0.285	6.763	0.299	0.47
	8.5	168.5	-22.36	4.54	-1.804	0.283	-0.275	0.282	0.167	0.293	-0.339	0.179	0.761	6.287	0.367	0.402
	9.5	167.5	-23.85	6.03	-1.164	-0.357	-0.782	0.789	-0.067	0.527	-0.321	0.161	-2.203	9.251	0.286	0.483
	9.5	168.5	-23.85	6.03	-1.564	0.043	-0.167	0.174	0.171	0.289	-0.421	0.261	-1.766	8.814	0.344	0.425
Majuro	6.5	170.5	2.316	-33.306	-0.517	-0.279	-0.11	0.267	0.064	-0.228	0.385	-0.742	4.834	-16.964	0.158	-0.179
	6.5	171.5	3.776	-34.766	-0.778	-0.018	0.028	0.129	-0.021	-0.143	0.703	-1.06	7.215	-19.345	0.216	-0.237
	7.5	170.5	-10.81	-20.18	-1.154	0.358	-0.21	0.367	-0.235	0.071	-0.039	-0.318	1.547	-13.677	0.173	-0.194
	7.5	171.5	-8.019	-22.971	-0.735	-0.061	0.035	0.122	0.146	-0.31	0.289	-0.646	3.035	-15.165	0.206	-0.227
American Samoa	-13.5	-170.5	-3.886	29.196	-2.118	4.282	-0.042	0.484	1.989	-1.972	0.282	-0.157	6.404	2.697	0.409	-0.451
	-13.5	-171.5	-1.7	27.01	-1.743	3.907	-0.017	0.459	1.243	-1.226	0.342	-0.217	8.326	0.775	0.474	-0.516
	-14.5	-170.5	1.867	23.443	-1.454	3.618	0.021	0.421	1.225	-1.208	0.271	-0.146	6.894	2.207	0.349	-0.391
	-14.5	-171.5	1.247	24.063	-2	4.164	0.182	0.26	0.435	-0.418	0.2	-0.075	6.268	2.833	0.336	-0.378
Pohnpei	6.5	157.5	-25.94	-46.92	-0.039	-0.003	-0.314	-0.014	0.039	0.118	-0.075	-0.514	-3.859	-17.651	0.055	-0.026
	6.5	158.5	-28.6	-44.26	-0.025	-0.017	-0.807	0.479	0.078	0.079	-0.5	-0.089	-3.634	-17.876	0.076	-0.047
	7.5	157.5	-36.71	-36.15	-0.16	0.118	-0.432	0.104	-0.092	0.249	-0.596	0.007	-5.537	-15.973	0.105	-0.076
	7.5	158.5	-32.15	-40.71	-0.86	0.818	-0.1	-0.228	0.228	-0.071	-0.635	0.046	-5.392	-16.118	0.078	-0.049
Yap	8.5	137.5	4.947	-29.547	0.36	-0.367	0.31	0.104	-0.121	0.388	0.235	-0.42	1.481	-10.403	0.006	0.004
	8.5	138.5	4.064	-28.664	-0.1	0.093	0.821	-0.407	0.067	0.2	0.292	-0.477	2.079	-11.001	0.035	-0.025
	9.5	137.5	-0.425	-24.175	0.81	-0.817	-0.232	0.646	-0.1	0.367	0.178	-0.363	1.598	-10.52	0.07	-0.06
	9.5	138.5	-2.904	-21.696	0.617	-0.624	0.803	-0.389	0.078	0.189	0.11	-0.295	1.943	-10.865	0.132	-0.122

up to 0.4 (0.432) days yr^{-1} on Chuuk. Differences between rain gauge and satellite observations is known to be high over the tropical Pacific Ocean (Bowman 2005), perhaps explaining the disparity in calculated trends seen in the current study. However, due to the spatial smoothing of the gridded data, caution should always be taken when comparing satellite or other gridded products and gauge-based data.

Another interesting result from Table 2 is the differences between GPCP and rain gauge-derived trends in these indicators being smaller at certain locations than others. Pohnpei consistently possessed low disagreement between these two means of rainfall trend computation, when compared to the other seven locations, for Rainfall Frequency, Maximum Dry Consecutive Days, Extreme Rainfall Frequency, and Extreme Rainfall Proportion. By contrast, locations such as Palau experienced frequently high disagreement, with differences in Extreme Rainfall Intensity and Extreme Rainfall Frequency being up to −35 (−34.547) mm yr^{-1} and -0.9 (−0.925) days yr^{-1} respectively. The most likely explanation for the difference is the small-scale stochastic rainfall variability in this region, although satellite errors, gridding, and management could all provide explanations for this spatial disparity in the differences between rain gauges and GPCP trends.

Whilst Table 2 communicates the discrepancies between rain gauge and GPCP-derived rainfall trends, it is of interest to know whether these differences vary at all by season, given the seasonality that rainfall indicators obtained from rain gauges were shown to possess in Section 3.2. Appendices A1, A2, A3, and A4 show the same analysis as that of Table 2 but instead for NH winter, spring, summer, and autumn respectively. These tables show some overall agreement that the differences between rain gauge and GPCP trends are somewhat smaller in NH spring for the majority of rainfall indicators, namely Rainfall Amount, Rainfall Frequency, and Maximum Dry/Wet Consecutive Days. However, the occurrence of low differences in NH spring is not consistently true, especially in the case of locations such as Yap, where the NH spring difference in Rainfall Amount can be as much as −20 (−19.619) mm yr^{-1}, compared to its much lower autumn difference of +6 (+6.42) mm yr^{-1}. This tendency for differences in calculated trends being smaller in NH spring is likely to be coincidental, but could also be related to the nature of rainfall patterns that occur over the tropical Pacific Ocean at this time, given the seasonal to interannual rainfall cycles that are associated with the ITCZ (Broccoli et al., 2006) and ENSO (Wang and Picaut 2004).

4. Discussion

The goal of the current study was to further previously conducted research concerning gauge-based tropical Pacific rainfall trends, such as Greene et al. (2007) and McGree et al. (2014). This work builds on these previous studies by applying a broad collection of rainfall indicators to rain gauge observations selected from the PACRAIN database on annual, seasonal, and monthly timescales, and subsequently compares the obtained results to satellite-derived products. This work also sought to consider the importance of climate variability cycles, and meteorological features, as factors that could offer explanations for the observed trends, and extend this analysis for newly available rainfall data. It seems from the results of the current study that much of the trends in rainfall indicators that have been observed in previous studies have continued, namely that decreases of Rainfall Amount and Rainfall Frequency, and increases in Maximum Dry Consecutive Days, have dominated in the tropical Pacific Ocean over the last few decades (Figs. 1–3; Greene et al., 2007; McGree et al., 2014). The continuation of these trends has happened despite the phase of the IPO shifting from positive to negative in the late 1990s, a process that has been associated previously with changes in rainfall patterns over the tropical Pacific Ocean, especially its western side (Salinger et al., 2001; Folland et al., 2002; Gouriou and Delcroix 2002). There was, however, some evidence of the IPO having a stronger influence on seasonal trends in these rainfall indicators, such as for NH summer Extreme Rainfall Intensity, based on the similarity between the trends observed in single IPO phases and the entire observational period (1971–2017, see Fig. 6d–f). In addition to this finding, an east-west spatial disparity in some rainfall indicators occurred in NH spring, with decreases of Extreme Rainfall Proportion (Fig. 5a–c) and Rainfall Amount (Fig. 5d–f) occurring to the east and west respectively. Meteorological features, such as the SPCZ, are known to vary in their latitudinal position due to changes in the state of the IPO and ENSO (Vincent et al., 2011), which could explain some of this spatial difference. However, what is more likely is that these particular results occurred by random chance, since the SPCZ tends to influence rainfall patterns instead over the southern half of the western tropical Pacific Ocean.

Despite previous studies attesting to the importance of the IPO in influencing multidecadal rainfall trends in the tropical Pacific Ocean, this influence is not clear across the region for the data analyzed here. Furthermore, given the small number of locations that had sufficient data completeness to be analyzed in this work, it is not possible to more than suggest that the IPO's influences on tropical Pacific rainfall patterns have been less important than expected in recent decades.

Breaking down changes in rainfall indicators by month seemed to reveal greater sensitivity to the processes known to influence tropical Pacific rainfall. Monthly time series plots constructed for individual locations (Fig. 8) illustrate an oscillating interannual variability in these indicators, superimposed onto a (usually negative) multidecadal trend, with many of these trends possessing statistical significance. El Niño events, based on the expected occurrence of above-average rainfall totals in the West Pacific (Wang and Picaut 2004), were occasionally detectable during NH spring months for Rainfall Amount (Fig. 8a), Maximum Dry Consecutive Days (Fig. 8h), and Extreme Rainfall Intensity (Fig. 8i). Such a result is consistent with previous expectations that ENSO is associated with detectable impacts on tropical Pacific rainfall, largely due to its impacts on features such as the ITCZ and SPCZ (Salinger et al., 2001; Folland et al., 2002; Xie et al., 2018).

The significance of ENSO for these monthly trends of rainfall indicators should, however, not be overstated, since its influences were frequently difficult to detect, as was the relevance of different IPO phases (Fig. 8). Despite the apparently minor influences of the IPO and ENSO on these trends (as was largely the case in analyzing their seasonal and annual trends), multidecadal decreases in monthly rainfall indicators were frequently exhibited, with all time-series charts in Fig. 8 possessing statistical significance ($p < 0.1$). This statistical significance, along with that seen in Figs. 1–7 (white triangles), is prevalent enough that it is worth considering what other climatic processes could offer explanations for them.

One possible process is climate change, with it being commonly accepted that increased global temperatures generally lead to less frequent but more powerful rainfall events (Trenberth 2011; Bindoff et al., 2013; Donat et al., 2016), evidence of which can somewhat be seen in Figs. 1–3 (higher Rainfall Amount, lower Maximum Dry Consecutive Days). Whilst changes in rainfall under climate change are likely to be small over these gauge locations, versus the larger projected increases over the Central/Eastern Tropical Pacific (Bell et al., 2013), ENSO-related rainfall in this region is expected to decrease in amount and become less variable (Huang and Xie 2015). The statistically significant negative trends in Fig. 8 suggest that decreases in ENSO-related rainfall might already be happening. The ITCZ, another process that influences tropical Pacific Rainfall, could also be affected by climate change, whether in terms of a narrowing of its convergence zone (Byrne and Schneider 2016) or a strengthening of its deep convection (Bony et al., 2013), perhaps contributing to increasing rainfall intensity over these islands.

However, caution should be taken when attributing climate change (or climate variability cycles) to the trends presented in this work. Physical reasons for this caution include the concern that rain gauge records do not accurately represent a wider region's rainfall patterns (Bell and Kundu 2003), the lack of consensus about the role of orography

in influencing rainfall over small islands (Griffiths et al., 2003; Hopuare et al., 2015), and the role of stochastic rainfall variability (e.g. tropical cyclones and isolated convection) in producing the observed trends (Greene et al., 2007). Moreover, the inconsistent sign of the statistically significant trends, despite these islands' relative proximity (Figs. 1–7), makes attribution challenging within the current study's scope, as does possessing data from only 8 rain gauges and a short GPCP data record. A comprehensive attribution study that links rain gauge-based tropical Pacific rainfall trends to climatic processes is therefore recommended as future work on this topic.

Finally, this study compared the rain gauge results with the annual and seasonal trends of the same seven rainfall indicators using GPCP observations (Table 2 and Appendix A1-4). What this comparison revealed was occasionally large discrepancies between rain gauge and GPCP-derived trends of the same indicators, with these discrepancies varying considerably when comparing trends computed at different locations. For instance, differences between the two datasets were relatively small at islands such as Pohnpei and Guam for indicators like Maximum Dry Consecutive Days and Extreme Rainfall Frequency, but then much larger for Palau when computing Rainfall Amount. Such large differences between rain gauge and GPCP-derived rainfall indicators are consistent with previous work that also found these differences to exist (Hughes 2006; Salio et al., 2015). A study of rain gauge versus satellite data comparison over the tropical Pacific Ocean by Bowman (2005) showed that, over several years of recorded observations, the root-mean-squared difference between these two means of measuring rainfall can be as much as 200–300%. Given the differing spatial scale of the two estimates, such large disparity over a wide area of the Pacific Ocean could partially explain why measured rainfall presented in the current study differs across locations.

The GPCP observations themselves do possess some agreement with previous studies of long-term satellite-derived rainfall trends. Kruk et al. (2015) showed that recent trends in tropical Pacific rainfall have been increases closer to the western boundary of the Pacific Ocean and decreases further away from coastlines. This finding shows some indication of having been replicated, especially when examining autumn increases in Rainfall Amount (Appendix A4) at more western locations (e.g. Palau and Yap) and comparing these to the decreasing trends found at locations to the east (e.g. American Samoa and Kwajalein). The GPCP trends produced in this work can therefore be verified to an extent. However, since satellite-derived rainfall trends were not a primary focus of the current study, the comparison of these trends against those derived from rain gauges was somewhat cursory. Future work could explore a more in-depth analysis of calculating multiple rainfall indicators from GPCP data, especially once enough years of data to assess satellite-derived rainfall climatology are available.

What the results from the current study have shown is that (occasionally statistically significant) reductions in the amount of rainfall and increases in the extremity of drought events have occurred at multiple islands and atolls across the tropical Pacific Ocean, resulting in up to hundreds of millimeters of annual rainfall lost when comparing the start and end of the period of study. The consequent effects on the economy and livelihoods of the inhabitants of these islands are of serious concern, especially if these reductions continue or exacerbate later into this century.

Author statement

Joshua Wimhurst: Methodology, Software, Writing- Original draft preparation, Visualization, Validation **John Scott Greene:** Conceptualization, Writing- Reviewing and Editing, Supervision.

Declaration of competing interest

The authors declare that they have no known competing financial interests or personal relationships that could have appeared to influence the work reported in this paper.

Acknowledgements

The authors of this work would like to thank the Grant ID: NA16OAR4320115, funded by the NOAA Climate Program Office for funding this research, as well as the meteorological institutes around the Pacific Ocean for providing data. Thanks are also given to Mr. Ethan Cook for providing support with data preparation and provision.

Appendices.

A1 *– Same as Table 2 but for winter trends in GPCP and rain gauge-derived rainfall indicators*

Station Name	Latitude	Longitude	Rainfall Amount (mm/yr)		Rainfall Frequency (days/yr)		Max. Consecutive Wet Days (days/yr)		Max. Consecutive Dry Days (days/yr)		Extreme Rainfall Frequency (days/yr)		Extreme Rainfall Intensity (mm/yr)		Extreme Rainfall Proportion (%/yr)	
			GPCP	Gauge-GPCP	GPCP	Gauge-GPCP	GPCP	Gauge-GPCP	GPCP	Gauge-GPCP	GPCP	Gauge-GPCP	GPCP	Gauge-GPCP	GPCP	Gauge-GPCP
Chuuk	6.5	151.5	-20.06	6.26	-0.257	-0.107	-0.132	0.004	0.067	0.15	-0.378	0.246	-3.909	-1.31	0.041	0.026
	6.5	152.5	-19.55	5.75	-0.246	-0.118	0.246	-0.374	0.15	0.067	-0.317	0.185	-3.903	-1.316	0.03	0.037
	7.5	151.5	-20.6	6.8	-0.285	-0.079	-0.303	0.175	0.032	0.185	-0.414	0.282	-4.206	-1.013	0.114	-0.047
	7.5	152.5	-20.33	6.53	-0.178	-0.186	-0.192	0.064	0.11	0.107	-0.389	0.257	-3.544	-1.675	0.176	-0.109
Guam	13.5	144.5	-9.068	-6.812	-0.385	0.577	-0.128	0.181	0.257	-0.332	-0.26	0.046	-3.431	-8.899	0.494	-1.239
	13.5	145.5	-8.406	-7.474	-0.5	0.692	-0.21	0.263	0.014	-0.089	-0.146	-0.068	-3.266	-9.064	0.429	-1.174
	14.5	144.5	-6.338	-9.542	-0.875	1.067	-0.046	0.099	0.264	-0.339	-0.175	-0.039	-2.877	-9.453	0.423	-1.168
	14.5	145.5	-7.233	-8.647	-0.814	1.006	-0.16	0.213	0.107	-0.182	-0.214	0	-3.073	-9.257	0.4	-1.145
Palau	6.5	133.5	2.033	-29.573	-0.507	0.404	0.214	-0.328	0.071	0.036	0.003	-0.313	2.023	-13.043	0.078	-0.408
	6.5	134.5	-1.297	-26.243	-0.317	0.214	0.357	-0.471	0.121	-0.014	0.003	-0.313	1.886	-12.906	0.168	-0.498
	7.5	133.5	-0.281	-27.259	-0.314	0.211	-0.153	0.039	0.078	0.029	0.078	-0.388	2.056	-13.076	0.278	-0.608
	7.5	134.5	-1.002	-26.538	-0.492	0.389	-0.325	0.211	0.271	-0.164	0.067	-0.377	1.911	-12.931	0.282	-0.612
Kwajalein	8.5	167.5	-4.337	-7.373	-0.835	0.035	-0.146	-0.1	0.332	-0.05	0.014	-0.271	1.231	-1.532	0.9	0.524
	8.5	168.5	-3.293	-8.417	-1.254	0.454	-0.275	0.029	0.314	-0.032	0.06	-0.317	2.745	-3.046	1.234	0.19
	9.5	167.5	-1.325	-10.385	-0.75	-0.05	-0.203	-0.043	0.225	0.057	0.107	-0.364	0.641	-0.942	0.515	0.909
	9.5	168.5	-2.149	-9.561	-0.785	-0.015	-0.267	0.021	0.114	0.168	0.057	-0.314	0.381	-0.682	0.528	0.896
Majuro	6.5	170.5	-10.12	-13.54	-0.628	-0.107	-0.307	0.136	0.221	-0.253	0.085	-0.277	1.969	-10.546	0.721	-0.38
	6.5	171.5	-10.42	-13.24	-0.782	0.047	-0.303	0.132	0.021	-0.053	0.128	-0.32	2.727	-11.304	0.775	-0.434
	7.5	170.5	-8.277	-15.383	-0.878	0.143	-0.467	0.296	0.121	-0.153	0.125	-0.317	1.177	-9.754	0.675	-0.334
	7.5	171.5	-7.923	-15.737	-0.792	0.057	-0.321	0.15	0.353	-0.385	0.142	-0.334	1.829	-10.406	0.75	-0.409
American Samoa	-13.5	-170.5	20.56	6.21	-0.178	0.963	0.114	0.403	0.242	-0.302	0.439	-0.239	5.39	2.201	0.092	-0.342
	-13.5	-171.5	22.78	3.99	-0.217	1.002	0.267	0.25	0.092	-0.152	0.435	-0.235	6.833	0.758	0.192	-0.442
	-14.5	-170.5	20.45	6.32	-0.039	0.824	0.228	0.289	0.035	-0.095	0.425	-0.225	5.9	1.691	0.106	-0.356
	-14.5	-171.5	21.9	4.87	-0.121	0.906	0.439	0.078	-0.167	0.107	0.489	-0.289	5.582	2.009	0.016	-0.266
Pohnpei	6.5	157.5	-17.83	-30.33	-0.55	0.286	-0.782	0.361	0.246	-0.136	-0.185	-0.207	-1.112	-12.318	0.429	-0.035
	6.5	158.5	-17.08	-31.08	-0.596	0.332	-0.682	0.261	0.253	-0.143	-0.175	-0.217	-0.549	-12.881	0.452	-0.058
	7.5	157.5	-22.23	-25.93	-0.735	0.471	-0.653	0.232	0.267	-0.157	-0.285	-0.107	-2.512	-10.918	0.664	-0.27
	7.5	158.5	-18.68	-29.48	-1.132	0.868	-0.289	-0.132	0.371	-0.261	-0.382	-0.01	-1.463	-11.967	0.594	-0.2
Yap	8.5	137.5	-8.17	5.43	-0.571	-0.082	-0.135	-0.04	-0.189	0.392	-1.209	1.219	-0.112	0.759	0.337	0.033
	8.5	138.5	-6.031	3.291	-0.607	-0.046	-0.153	-0.022	-0.042	0.245	0.103	-0.093	0.177	0.47	0.268	0.102
	9.5	137.5	-8.614	5.874	-0.153	-0.5	0.135	-0.31	0.014	0.189	-0.182	0.192	-1.048	1.695	0.262	0.108
	9.5	138.5	-8.039	5.299	-0.078	-0.575	0.035	-0.21	0.067	0.136	-0.164	0.174	-1.121	1.768	0.247	0.123

A2 *– Same as Table 2 but for spring trends in GPCP and rain gauge-derived rainfall indicators*

Station Name	Latitude	Longitude	Rainfall Amount (mm/yr)		Rainfall Frequency (days/yr)		Max. Consecutive Wet Days (days/yr)		Max. Consecutive Dry Days (days/yr)		Extreme Rainfall Frequency (days/yr)		Extreme Rainfall Intensity (mm/yr)		Extreme Rainfall Proportion (%/yr)	
			GPCP	Gauge-GPCP	GPCP	Gauge-GPCP	GPCP	Gauge-GPCP	GPCP	Gauge-GPCP	GPCP	Gauge-GPCP	GPCP	Gauge-GPCP	GPCP	Gauge-GPCP
Chuuk	6.5	151.5	-9.069	-4.711	-0.003	-0.4	-0.375	0.022	-0.082	0.099	-0.028	-0.043	-0.566	-1.455	0.122	0.204
	6.5	152.5	-5.698	-8.082	0.042	-0.445	-0.078	-0.275	-0.192	0.209	0.025	-0.096	0.47	-2.491	0.164	0.162
	7.5	151.5	-9.3	-4.48	-0.225	-0.178	-0.303	-0.05	3.518	-3.501	-0.15	0.079	-0.457	-1.564	0.212	0.114
	7.5	152.5	-8.172	-5.608	-0.132	-0.271	-0.196	-0.157	-0.135	0.152	-0.2	0.129	0.287	-2.308	0.282	0.044
Guam	13.5	144.5	0.842	1.772	-0.432	0.489	-0.982	0.157	-0.05	-0.025	0.014	0.168	2.14	-1.335	0.921	-0.845
	13.5	145.5	0.249	2.365	-0.5	0.557	0.146	0.029	-0.292	0.217	0.035	0.147	2.033	-1.228	0.945	-0.869
	14.5	144.5	1.685	0.929	-0.739	0.796	0.082	0.093	0.164	-0.239	0.189	-0.007	2.024	-1.219	0.504	-0.428
	14.5	145.5	1.144	1.47	-0.467	0.524	0.075	0.1	0.385	-0.46	0.078	0.104	2.016	-1.211	0.692	-0.616
Palau	6.5	133.5	-2.38	-4.239	0.317	0.208	-0.217	-0.14	-0.239	0.111	-0.064	0.103	-0.586	-3.207	-0.014	-0.129
	6.5	134.5	-5.699	-0.92	0.317	0.208	-0.317	-0.04	-0.132	0.004	-0.242	0.281	-1.481	-2.312	-0.037	-0.106
	7.5	133.5	-6.033	-0.586	-0.046	0.571	-0.021	-0.336	-0.196	0.068	-0.242	0.281	-1.524	-2.269	-0.003	-0.14
	7.5	134.5	-7.417	0.798	0.117	0.408	-0.271	-0.086	-0.142	0.014	-0.139	0.178	-1.201	-2.592	0.072	-0.215
Kwajalein	8.5	167.5	-2.141	6.727	0.107	-0.257	-0.078	0.053	-0.285	0.613	-0.114	0.192	1.011	3.769	0.316	0.762
	8.5	168.5	-4.005	8.591	0.142	-0.292	-0.103	0.078	-0.182	0.51	-0.246	0.324	-0.402	5.182	0.038	1.04
	9.5	167.5	-2.778	7.364	0.117	-0.267	-0.046	0.021	0.278	0.05	-0.103	0.181	-0.387	5.167	-0.237	1.315
	9.5	168.5	-1.764	6.35	0.21	-0.36	0.096	-0.121	0.182	0.146	-0.021	0.099	-0.961	5.741	-0.591	1.669
Majuro	6.5	170.5	9.454	-5.547	0.221	-0.15	-0.453	0.143	-0.25	0.079	0.182	-0.157	1.742	4.913	-0.123	0.82
	6.5	171.5	8.731	-4.824	0.167	-0.096	0.025	-0.335	-0.175	0.004	0.289	-0.264	2.635	4.02	0.013	0.684
	7.5	170.5	0.83	3.077	0.135	-0.064	-0.096	-0.214	-0.321	0.15	0.014	0.011	0.133	6.522	-0.101	0.798
	7.5	171.5	2.403	1.504	0.16	-0.089	-0.085	-0.225	-0.221	0.05	0.167	-0.142	0.995	5.66	-0.034	0.731
American Samoa	-13.5	-170.5	-16.33	-1.91	-0.342	0.82	-0.132	0.185	0.264	-0.211	-0.235	0.157	-4.226	-8.244	0.436	-0.972
	-13.5	-171.5	-12.76	-5.48	-0.114	0.592	-0.235	0.288	0.425	-0.372	-0.021	-0.057	-3.297	-9.173	0.376	-0.912
	-14.5	-170.5	-11.43	-6.81	-0.01	0.488	-0.207	0.26	0.167	-0.114	-0.132	0.054	-2.909	-9.561	0.317	-0.853
	-14.5	-171.5	-10.65	-7.59	-0.382	0.86	-0.296	0.349	0.035	0.018	-0.05	-0.028	-3.255	-9.215	0.318	-0.854
Pohnpei	6.5	157.5	-9.25	-20.13	-0.071	-0.232	-0.585	-0.147	0.057	0.353	0.032	-0.232	-0.249	-4.812	0.204	0.083
	6.5	158.5	-9.296	-20.084	-0.075	-0.228	-1.061	0.329	0.003	0.407	-0.035	-0.165	-0.333	-4.728	0.2	0.087
	7.5	157.5	-6.66	-22.72	-0.146	-0.157	-0.828	0.096	-0.157	0.567	-0.01	-0.19	1.205	-6.266	0.44	-0.153
	7.5	158.5	-5.696	-23.684	-0.064	-0.239	-0.621	-0.111	-0.017	0.427	0.046	-0.246	0.527	-5.588	0.311	-0.024
Yap	8.5	137.5	-8.178	-17.452	0.196	-0.317	-0.214	0	-0.228	0.363	-0.078	-0.325	-1.228	-11.692	0.083	-0.316
	8.5	138.5	-6.011	-19.619	0.196	-0.146	-0.325	0.111	-0.05	0.185	0.007	-0.41	-0.474	-12.446	0.11	-0.343
	9.5	137.5	-6.363	-19.267	0.196	-0.478	-0.585	0.371	-0.192	0.327	-0.107	-0.296	-0.704	-12.216	0.272	-0.505
	9.5	138.5	-6.64	-18.99	0.196	-0.104	-0.339	0.125	-0.139	0.274	0.075	-0.478	-0.494	-12.426	0.328	-0.561

A3 *– Same as Table 2 but for summer trends in GPCP and rain gauge-derived rainfall indicators*

Station Name	Latitude	Longitude	Rainfall Amount (mm/yr)		Rainfall Frequency (days/yr)		Max. Consecutive Wet Days (days/yr)		Max. Consecutive Dry Days (days/yr)		Extreme Rainfall Frequency (days/yr)		Extreme Rainfall Intensity (mm/yr)		Extreme Rainfall Proportion (%/yr)	
			GPCP	Gauge-GPCP	GPCP	Gauge-GPCP	GPCP	Gauge-GPCP	GPCP	Gauge-GPCP	GPCP	Gauge-GPCP	GPCP	Gauge-GPCP	GPCP	Gauge-GPCP
Chuuk	6.5	151.5	-5.113	10.965	0.135	0.297	-0.267	0.542	-0.035	0.052	0.025	0.157	-1.379	-0.448	0.011	-0.072
	6.5	152.5	-1.52	7.372	-0.039	0.471	-0.371	0.646	-0.075	0.092	-0.028	0.21	-0.869	-0.958	0	-0.061
	7.5	151.5	-7.463	13.315	0.2	0.232	-0.507	0.782	-0.05	0.067	-0.157	0.339	-2.204	0.377	-0.039	-0.022
	7.5	152.5	-8.659	14.511	-0.085	0.517	-0.585	0.86	-0.042	0.059	-0.103	0.285	-2.106	0.279	0.016	-0.077
Guam	13.5	144.5	-11.87	-10.98	-0.439	0.147	0.01	-0.374	0.25	-0.175	-0.214	0.086	-3.114	-1.972	0.012	0.252
	13.5	145.5	-12.09	-10.76	-0.342	0.05	0.014	-0.378	0.471	-0.396	-0.182	0.054	-3.346	-1.74	0.066	0.198
	14.5	144.5	-8.35	-14.5	-0.203	-0.089	0.06	-0.424	0.264	-0.189	-0.028	-0.1	-2.269	-2.817	0.129	0.135
	14.5	145.5	-6.682	-16.168	-0.4	0.108	0.003	-0.367	0.217	-0.142	-0.125	-0.003	-2.978	-2.108	-0.135	0.399
Palau	6.5	133.5	9.925	-26.585	0.671	0.425	0.092	0.283	-0.296	0.114	-0.042	-0.3	-1.211	-14.539	-0.346	-0.494
	6.5	134.5	3.936	-20.596	0.61	0.486	-1.506	1.881	-0.221	0.039	-0.146	-0.196	-2.21	-13.54	-0.321	-0.519
	7.5	133.5	0.364	-17.024	0.232	0.864	0.307	0.068	-0.189	0.007	-0.089	-0.253	-0.923	-14.827	-0.118	-0.722
	7.5	134.5	-2.061	-14.599	0.253	0.843	-0.271	0.646	-0.16	-0.022	-0.228	-0.114	-1.89	-13.86	-0.169	-0.671
Kwajalein	8.5	167.5	-8.17	-5.44	-0.328	-0.05	-0.417	0.4	-0.035	0.052	-0.11	0.007	-1.245	-0.89	0.109	0.297
	8.5	168.5	-9.315	-4.295	-0.61	0.232	-0.282	0.265	0.028	-0.011	-0.207	0.104	-0.248	-1.887	0.327	0.079
	9.5	167.5	-10.86	-2.75	-0.414	0.036	-0.575	0.558	-0.017	0.034	-0.328	0.225	-1.098	-1.037	0.288	0.118
	9.5	168.5	-11.95	-1.66	-0.592	0.214	-0.246	0.229	-0.075	0.092	-0.35	0.247	-0.95	-1.185	0.411	-0.005
Majuro	6.5	170.5	-1.07	-1.432	-0.121	0.167	-0.314	0.15	-0.067	0.102	0.071	-0.004	1.028	-2.432	0.21	-0.251
	6.5	171.5	-0.66	-1.842	-0.353	0.399	-0.21	0.046	-0.057	0.092	0.171	-0.104	1.067	-2.471	0.193	-0.234
	7.5	170.5	-4.376	1.874	-0.257	0.303	-0.492	0.328	-0.06	0.095	-0.171	0.238	-0.513	-0.891	0.087	-0.128
	7.5	171.5	-5.137	2.635	-0.178	0.224	-0.339	0.175	-0.021	0.056	-0.092	0.159	0.195	-1.599	0.225	-0.266
American Samoa	-13.5	-170.5	3.401	9.129	-0.685	1.485	0.107	0.15	1.161	-1.364	0.164	-0.161	1.697	5.343	0.995	-1.123
	-13.5	-171.5	2.274	10.256	-0.578	1.378	0.032	0.225	0.539	-0.742	0.135	-0.132	0.649	6.391	0.625	-0.753
	-14.5	-170.5	3.449	9.081	-0.653	1.453	0.028	0.229	1.139	-1.342	0.16	-0.157	1.704	5.336	0.752	-0.88
	-14.5	-171.5	2.948	9.582	-0.882	1.682	0.121	0.136	0.217	-0.42	0.203	-0.2	1.818	5.222	0.868	-0.996
Pohnpei	6.5	157.5	-5.147	-3.517	0.092	0.175	-0.078	0.195	-0.042	-0.033	-0.146	0	-1.184	-2.452	0	-0.031
	6.5	158.5	-4.937	-3.727	0.175	0.092	0.039	0.078	0.042	-0.117	-0.307	0.161	-0.988	-2.648	0.008	-0.039
	7.5	157.5	-11.1	2.436	0.185	0.082	-0.26	0.377	0.003	-0.078	-0.25	0.104	-2.947	-0.689	-0.096	0.065
	7.5	158.5	-9.356	0.692	0.032	0.235	0.225	-0.108	-0.017	-0.058	-0.196	0.05	-1.707	-1.929	0.065	-0.096
Yap	8.5	137.5	-10.44	-16.69	0.171	0.261	0.625	-0.258	-0.05	0.064	-0.328	0.089	-3.285	-5.586	-0.146	0.134
	8.5	138.5	-10.42	-16.71	-0.025	0.457	0.832	-0.465	-0.082	0.096	-0.253	0.014	-3.02	-5.851	-0.126	0.114
	9.5	137.5	-13.78	-13.35	0.16	0.272	-0.1	0.467	0.064	-0.05	-0.332	0.093	-2.885	-5.986	-0.043	0.031
	9.5	138.5	-13.66	-13.47	0.235	0.197	0.21	0.157	0.032	-0.018	-0.3	0.061	-2.894	-5.977	-0.028	0.016

A4 – *Same as Table 2 but for autumn trends in GPCP and rain gauge-derived rainfall indicators*

Station Name	Latitude	Longitude	Rainfall Amount (mm/yr)		Rainfall Frequency (days/yr)		Max. Consecutive Wet Days (days/yr)		Max. Consecutive Dry Days (days/yr)		Extreme Rainfall Frequency (days/yr)		Extreme Rainfall Intensity (mm/yr)		Extreme Rainfall Proportion (%/yr)	
			GPCP	Gauge-GPCP	GPCP	Gauge-GPCP	GPCP	Gauge-GPCP	GPCP	Gauge-GPCP	GPCP	Gauge-GPCP	GPCP	Gauge-GPCP	GPCP	Gauge-GPCP
Chuuk	6.5	151.5	13.76	-9.289	0.578	-0.35	0.114	0.161	-0.192	0.231	0.321	-0.2	2.622	-1.098	-0.05	0.034
	6.5	152.5	13.12	-8.649	0.7	-0.472	-0.035	0.31	-0.21	0.249	0.239	-0.118	1.328	0.196	-0.204	0.188
	7.5	151.5	11.19	-6.719	0.607	-0.379	0.657	-0.382	0.007	0.032	0.203	-0.082	1.563	-0.039	-0.099	0.083
	7.5	152.5	10.2	-5.729	0.492	-0.264	0.178	0.097	-0.057	0.096	0.164	-0.043	1.432	0.092	-0.089	0.073
Guam	13.5	144.5	11.78	7.94	0.357	-0.396	0.235	-0.193	0.25	-0.307	0.189	0.089	2.353	6.771	-0.198	0.191
	13.5	145.5	10.72	9	0.235	-0.274	0.728	-0.686	0.325	-0.382	0.164	0.114	1.074	8.05	-0.296	0.289
	14.5	144.5	14.35	5.37	0.189	-0.228	0.385	-0.343	-0.028	-0.029	0.3	-0.022	2.928	6.196	-0.261	0.254
	14.5	145.5	11.16	8.56	0.1	-0.139	0.042	0	0.3	-0.357	0.21	0.068	2.267	6.857	-0.172	0.165
Palau	6.5	133.5	23.37	-7.61	0.3	0.642	0.342	0.55	-0.103	-0.107	0.392	-0.364	4.043	-0.698	-0.385	0.034
	6.5	134.5	26.2	-10.44	0.567	0.375	0.503	0.389	-0.1	-0.11	0.417	-0.389	4.161	-0.816	-0.41	0.059
	7.5	133.5	21.43	-5.67	0.321	0.621	0.378	0.514	0.039	-0.249	0.46	-0.432	3.9	-0.555	-0.286	-0.065
	7.5	134.5	25.23	-9.47	0.132	0.81	0.182	0.71	-0.103	-0.107	0.442	-0.414	3.901	-0.556	-0.407	0.056
Kwajalein	8.5	167.5	-4.952	7.938	-0.267	0.15	0.107	-0.121	0.064	-0.124	-0.075	0.196	-0.641	3.844	0.157	0.18
	8.5	168.5	-5.227	8.213	-0.096	-0.021	-0.325	0.311	-0.007	-0.053	-0.203	0.324	-0.954	4.157	0.129	0.208
	9.5	167.5	-8.766	11.752	-0.164	0.047	-0.292	0.278	-0.082	0.022	-0.157	0.278	-2.109	5.312	0.11	0.227
	9.5	168.5	-7.844	10.83	-0.446	0.329	0.035	-0.049	-0.107	0.047	-0.007	0.128	-1.105	4.308	0.264	0.073
Majuro	6.5	170.5	3.434	-11.637	0.071	-0.299	0.321	0.064	-0.107	1.204	0.107	-0.289	0.278	-5.519	-0.057	-0.181
	6.5	171.5	5.457	-13.66	0.185	-0.413	0.378	0.007	-0.05	1.147	0.2	-0.382	0.191	-5.432	-0.104	-0.134
	7.5	170.5	1.118	-9.321	-0.107	-0.121	0.414	-0.029	0.114	0.983	0.046	-0.228	0.259	-5.5	0.062	-0.3
	7.5	171.5	2.421	-10.624	0.089	-0.317	0.192	0.193	0.028	1.069	0.05	-0.232	-0.203	-5.038	-0.06	-0.178
American Samoa	-13.5	-170.5	-11.96	14.77	-1	1.017	-0.167	0.238	0.757	-0.778	-0.185	-1.013	-2.399	7.174	0.192	0.226
	-13.5	-171.5	-14.01	16.82	-0.885	0.902	-0.264	0.335	0.728	-0.749	-0.228	-0.97	-2.763	7.538	0.25	0.168
	-14.5	-170.5	-11.16	13.97	-0.792	0.809	-0.128	0.199	0.228	-0.249	-0.157	-1.041	-1.777	6.552	0.17	0.248
	-14.5	-171.5	-13.03	15.84	-0.639	0.656	-0.103	0.174	0.475	-0.496	-0.292	-0.906	-2.198	6.973	0.239	0.179
Pohnpei	6.5	157.5	4.594	6.046	0.482	-0.286	0.1	0.25	-0.31	0.1	-0.042	0.095	-0.942	3.795	-0.235	0.237
	6.5	158.5	1.769	8.871	0.446	-0.25	0.182	0.168	-0.228	0.018	-0.053	0.106	-0.9	3.753	-0.141	0.143
	7.5	157.5	1.981	8.659	0.507	-0.311	0.56	-0.21	-0.328	0.118	-0.06	0.113	-1.083	3.936	-0.205	0.207
	7.5	158.5	0.701	9.939	0.317	-0.121	0.478	-0.128	-0.325	0.115	-0.153	0.206	-1.911	4.764	-0.267	0.269
Yap	8.5	137.5	32.16	-0.16	0.55	-0.229	0.296	-0.139	0.071	-0.036	0.55	-0.143	5.438	5.862	-0.321	0.361
	8.5	138.5	26.77	5.23	0.507	-0.186	0.503	-0.346	0.16	-0.125	0.496	-0.089	3.926	7.374	-0.347	0.387
	9.5	137.5	28.29	3.71	0.471	-0.15	0.364	-0.207	0.21	-0.175	0.417	-0.01	5.276	6.024	-0.277	0.317
	9.5	138.5	25.58	6.42	0.492	-0.171	1.021	-0.864	0.132	-0.097	0.55	-0.143	5.401	5.899	-0.176	0.216

References

Adler, R.F., Huffam, G.J., Bolvin, D.T., Curtis, S., Nelkin, E.J., 2000. Tropical rainfall distributions determined using TRMM combined with other satellite and rain gauge information. J. Appl. Meteorol. 39, 2007–2023.

Adler, R.F., Huffman, G.J., Chang, A., Ferraro, R., Xie, P., Janowiak, J., Rudolf, B., Schnieder, U., Curtis, S., Bolvin, D., Gruber, A., Susskind, J., Arkin, P., Nelkin, E., 2003. The version-2 global precipitation climatology Project (GPCP) monthly precipitation analysis (1979-present). J. Hydrometeorol. 4, 1147–1167.

Bell, T.L., Kundu, P.K., 2003. Comparing satellite rainfall estimate with rain-gauge data: optimal strategies suggested by a spectral model. J. Geophys. Res. 108, 7-1–7-15.

Bell, J.D., Ganachaud, A., Gehrke, P.C., Griffiths, S.P., Hobday, A.J., Hoegh-Guldberg, O., Johnson, J.E., Le Borgne, R., Lehody, P., Lough, J.M., Matear, R.J., Pickering, T.D., Pratchett, M.S., Gupta, A.S., Senina, I., Waycott, M., 2013. Mixed responses of

tropical Pacific fisheries and aquaculture to climate change. Nat. Clim. Change 3, 591–599.
Bindoff, N.L., Stott, P.A., AchutaRao, K.M., Allen, M.R., Gillett, N., Gutzler, D., Hansingo, K., Hegerl, G., Hu, Y., Jain, S., Mokhov II, Overland, J., Perlwitz, J., Sebbari, R., Zhang, X., 2013. Detection and attribution of climate change: from global to regional. In: Stocker, T.F., Qin, D., Plattner, G.-K., Tignor, M., Allen, S.K., Boschung, J., Nauels, A., Xia, Y., Bex, V., Midgley, P.M. (Eds.), Climate Change 2013: the Physical Science Basis. Contribution of Working Group I to the Fifth Assessment Report of the Intergovernmental Panel on Climate Change. Cambridge University Press, Cambridge, United Kingdom and New York, NY, USA.
Bony, S., Bellon, G., Klocke, D., Sherwood, S., Fermepin, S., Denvil, S., 2013. Robust direct effect of carbon dioxide on tropical circulation and regional precipitation. Nat. Geosci. 6, 447–451.
Bowman, K.P., 2005. Comparison of TRMM precipitation retrievals with rain gauge data from ocean Buoys. J. Clim. 18, 178–190.
Broccoli, A.J., Dahl, K.A., Stouffer, R.J., 2006. Response of the ITCZ to northern Hemisphere cooling. Geophys. Res. Lett. 33, 4.
Byrne, M.P., Schneider, T., 2016. Narrowing of the ITCZ in a warming climate: physical mechanisms. Geopyhs Res Lett 43, 11350–11357.
Clark, S.K., Ming, Y., Held, I.M., Phillipps, P.J., 2018. The role of water vapor feedback in the ITCZ response to hemispherically asymmetric forcings. J. Clim. 31, 3659–3678.
Cook, W.E., Greene, J.S., 2019. Gridded monthly rainfall estimates derived from historical atoll observations. J. Atmos. Ocean. Technol. 36, 671–687.
Donat, M.G., Lowry, A.L., Alexander, L.V., O'Gorman, P.A., Maher, N., 2016. More extreme precipitation in the world's dry and wet regions. Nat. Clim. Change 6, 508–513.
ESRI, 2018. "Ocean base" [basemap]. Scale not given. "World ocean base". March 28, 2018. http://www.arcgis.com/home/item.html?id=1e126e7520f9466c9ca28b8f28b5e500.
Folland, C.K., Renwick, J.A., Salinger, M.J., Mullan, A.B., 2002. Relative influences of the interdecadal Pacific oscillation and ENSO on the south Pacific convergence zone. Geophys. Res. Lett. 29, 21-1-214.
Frazier, A.G., Giambelluca, T.W., 2016. Spatial trend analysis of Hawaiian rainfall from 1920 to 2012. Int. J. Climatol. 37, 2522–2531.
Gouriou, Y., Delcroix, T., 2002. Seasonal and ENSO variations of sea surface salinity and temperature in the South Pacific Convergence Zone during 1976-2000. J. Geophys. Res. 107. SRF 12-1 – SRF 12-14.
Greene, J.S., Paris, B., Morrissey, M., 2007. Historical changes in extreme precipitation events in the tropical Pacific region. Clim. Res. 34, 1–14.
Greene, J.S., Klatt, M., Morrissey, M., Postawko, S., 2008. The comprehensive Pacific rainfall database. J. Atmos. Ocean. Technol. 25, 71–82.
Griffiths, G.M., Salinger, M.J., Leleu, I., 2003. Trends in extreme daily rainfall across the south Pacific and relationship to the south Pacific convergence zone. Int. J. Climatol. 23, 847–869.
Hopuare, M., Pontaud, M., Céron, J.P., Ortéga, P., Laurent, V., 2015. Climate change, Pacific climate drivers and observed precipitation variability in Tahiti, French Polynesia. Clim. Res. 63, 157–170.
Huang, P., Xie, S.P., 2015. Mechanisms of change in ENSO-induced tropical Pacific rainfall variability in a warming climate. Nat. Geosci. 8, 922–926.
Huffman, G.J., Adler, R.F., Arkin, P., Chang, A., Ferraro, R., Gruber, A., Janowiak, J., McNab, A., Rudolf, B., Schneider, U., 1997. The global precipitation climatology Project (GPCP) combined precipitation dataset. Bull. Am. Meteorol. Soc. 78, 5–20.
Hughes, D.A., 2006. Comparison of satellite rainfall data with observations from gauging location networks. J. Hydrol. 327, 399–410.
Janowiak, J.E., Arkin, P.A., Morrissey, M., 1994. An examination of the diurnal cycle in oceanic tropical rainfall using satellite and in situ data. Mon. Weather Rev. 122, 2296–2311.
Kang, S.M., Held, I.M., Frierson, D.M., Zhao, M., 2008. The response of the ITCZ to extratropical thermal forcing: idealized slab-ocean experiments with a GCM. J. Clim. 21, 3521–3532.
Kim, D., Lee, S.K., Lopez, H., Goes, M., 2020. Pacific mean-state control of Atlantic multidecadal oscillation–El Niño relationship. J. Clim. 33, 4273–4291.
King, A.D., Alexander, L.V., Donat, M.G., 2013. The efficacy of using gridded data to examine extreme rainfall characteristics: a case study for Australia. Int. J. Climatol. 33, 376–2387.
Kruk, M.C., Lorrey, A.M., Griffiths, G.M., Lander, M., Gibney, E.J., Diamond, H.J., Marra, J.J., 2014. Review –On the state of the knowledge of rainfall extremes in the western and north Pacific basin. Int. J. Climatol. 35, 321–336.
Kruk, M.C., Hilburn, K., Marra, J.J., 2015. Using microwave satellite data to assess changes in storminess over the Pacific Ocean. Mon. Weather Rev. 143, 3214–3229.
Kumar, A., Chen, M., 2017. What is the variability in US west coast winter precipitation during strong El Niño events? Clim. Dynam. 49, 2789–2802.
Lavoie, R.L., 1963. Some aspects of the meteorology of the tropical Pacific viewed from an atoll. Atoll Res. Bull. 96, 1–80.
Li, X., Wang, X., Babovic, V., 2018. Analysis of variability and trends of precipitation extremes in Singapore during 1980-2013. Int. J. Climatol. 38, 125–141.
Luchetti, N.T., Sutton, J.R.P., Wright, E.E., Kruk, M.C., Marra, J.J., 2016. When El Niño rages: how satellite data can help water-stressed islands. Bull. Am. Meteorol. Soc. 97, 2249–2255.
Maggioni, V., Meyers, P.C., Robinson, M.D., 2016. A review of merged high-resolution satellite precipitation product accuracy during the tropical rainfall measuring mission (TRMM) era. J. Hydrometeorol. 17, 1101–1117.
McGree, S., Whan, K., Jones, D., Alexander, L.V., Imielska, A., Diamond, H., Ene, E., Finaulahi, S., Inape, K., Jacklick, L., Kumar, R., Laurent, V., Malala, H., Malsale, P., Moniz, T., Ngeaes, M., Peltier, A., Porteous, A., Pulehetoa-Mitiepo, R., Seuseu, S., Skilling, E., Tahani, L., Teimitsi, F., Toorua, U., Vaiimene, M., 2014. An updated assessment of trends and variability in total and extreme rainfall in the western Pacific. Int. J. Climatol. 34, 2775–2791.
McGree, S., Schreider, S., Kuleshov, Y., 2016. Trends and variability in droughts in the Pacific islands and northeast Australia. J. Clim. 29, 8377–8397.
Meehl, G.A., Hu, A., Arblaster, J.M., Fasullo, J., Trenberth, K.E., 2013. Externally forced and internally generated decadal climate variability associated with the Interdecadal Pacific Oscillation. J. Clim. 26, 7298–7310.
Meehl, G.A., Hu, A., Teng, H., 2016. Initialized decadal prediction for transition to positive phase of the Interdecadal Pacific Oscilllation. Nat. Commun. 11, 7.
Morrissey, M.L., Graham, N.E., 1996. Recent trends in rain gauge precipitation measurements from the tropical Pacific: evidence for an enhanced hydrologic cycle. Bull. Am. Meteorol. Soc. 77, 1207–1220.
Morrissey, M.L., Krajewski, W.F., McPhaden, M.J., 1994. Estimating rainfall in the tropics using the fractional time raining. J Appl Meteorol Clim 33, 387–393.
NASA TRMM, 2015. Tropical Rainfall Measuring Mission Homepage. https://pmm.nasa.gov/TRMM.
Morrissey, M.L., Shafer, M.A., Postawko, S.E., Gibson, B., 1995. The Pacific rain gage rainfall database. Water Resour. Res. 31, 2111–2113.
PACRAIN, 2018. PACRAIN – the Pacific Rainfall Database. http://pacrain.ou.edu/.
Postawko, S.E., Morrissey, M., Gibson, B., 1994. The schools of the Pacific Rainfall Climate Experiment: combining research and education. Bull. Am. Meteorol. Soc. 75, 1260–1266.
Raymond, D.J., Raga, G.B., Bretherton, C.S., López-Carrillo, C., Fuchs, Z., 2003. Convective forcing in the intertropical convergence zone of the eastern Pacific. J. Atmos. Sci. 60, 2064–2082.
Raymond, D.J., Bretherton, C.S., Molinari, J., 2006. Dynamics of the intertropical convergence zone of the east Pacific. J. Atmos. Sci. 63, 582–597.
Salinger, M.J., Basher, R.E., Fitzharris, B.B., Hay, J.E., Jones, P.D., Macveigh, J.P., Schmidely-Leleu, I., 1995. Climate trends in the south-west Pacific. Int. J. Climatol. 15, 285–302.
Salinger, M.J., Renwick, J.A., Mullan, A.B., 2001. Interdecadal Pacific oscillation and South Pacific climate. Int. J. Climatol. 21, 1705–1721.
Salio, P., Hobouchian, M.P., Skabar, Y.G., Vila, D., 2015. Evaluation of high-resolution satellite precipitation estimates over southern South America using a dense rain gauge network. Atmos. Res. 163, 146–161.
Schneider, T., Bischoff, T., Haug, G.H., 2014. Migrations and dynamics of the intertropical convergence zone. Nature 513, 45–53.
Sorooshian, S., Gao, X., Hsu, K., Maddox, R.A., Hong, Y., Gupta, H.V., Imam, B., 2002. Diurnal variability of tropical rainfall retrieved from combined GOES and TRMM satellite information. J. Clim. 15, 983–1001.
Sun, Q., Miao, C., Duan, Q., Ashouri, H., Sorooshian, S., Hsu, K.L., 2018. A review of global precipitation data sets: data sources, estimation, and intercomparisons. Rev. Geophys. 56, 79–107.
Trenberth, K.E., 2011. Changes in precipitation with climate change. Clim. Res. 47, 123–138.
Vincent, E.M., Lengaigne, M., Menkes, C.E., Jourdain, N.C., Marchesiello, P., Madec, G., 2011. Interannual variability of the South Pacific Convergence Zone and implications for tropical cyclone genesis. Clim. Dynam. 36, 1881–1896.
Wang, C., Picaut, J., 2004. Understanding ENSO physics – a review. Geophys. Monogr. 147, 21–48.
World Meteorological Organization, 2011. Commission for Climatology – over Eighty Years of Service. http://www.wmo.int/pages/prog/wcp/ccl/documents/WMO1079_web.pdf.
Xie, S., Peng, Q., Kamae, Y., Zheng, X., Tokinaga, H., Wang, D., 2018. Eastern Pacific ITCZ dipole and ENSO diversity. J. Clim. 31, 4449–4462.
Yue, S., Pilon, P., Cavadias, C., 2002. Power of the Man-Kendall and Spearman's rho tests for detecting monotonic trends in hydrological series. J. Hydrol. 259, 254–271.